R. SENA TÜRKER

DOCTORAL PROGRAM IN NEUROSCIENCE

DOCTOR OF PHILOSOPHY THESIS

2022

T.C.

YEDİTEPE UNIVERSITY
INSTITUTE OF HEALTH SCIENCES
DOCTORAL PROGRAM IN NEUROSCIENCE

MORPHOLOGICAL AND FUNCTIONAL EVALUATION OF 10-HYDROXY-2-DECENOIC ACID'S REGENERATIVE EFFECT ON MOUSE SCIATIC NERVE CRUSH MODEL

DOCTOR OF PHILOSOPHY THESIS

RABİA SENA TÜRKER

İstanbul-2022

T.C.

YEDİTEPE UNIVERSITY
INSTITUTE OF HEALTH SCIENCES
DOCTORAL PROGRAM IN NEUROSCIENCE

MORPHOLOGICAL AND FUNCTIONAL EVALUATION OF 10-HYDROXY-2-DECENOIC ACID'S REGENERATIVE EFFECT ON MOUSE SCIATIC NERVE CRUSH MODEL

DOCTOR OF PHILOSOPHY THESIS

RABİA SENA TÜRKER

SUPERVISOR

Prof. Dr. Bayram YILMAZ

İstanbul-2022

THESIS APPROVAL FORM

Institute : Yeditepe University Institute of Health Sciences

Programme : Neuroscience PhD Programme

Title of the Thesis : Morphological and Functional Evaluation Of 10-Hydroxy-2-Decenoic Acid's Regenerative Effect on Mouse Sciatic Nerve Crush Model

Owner of the Thesis : Rabia Sena Türker

Examination Date : 26.05.2022

This study has been approved as a Doctorate Thesis in regard to content and quality by the Jury.

Chair of the Jury:	Title, Name-Surname (Institution)	(Signature)
Supervisor:	Prof Dr, Bayram Yılmaz (Yeditepe University Institute of Health Sciences)	(Signature)
Co-supervisor:	Assoc Prof Dr, Ramazan Üstün (Van Yüzüncü Yıl University Faculty of Medicine)	(Signature)
Member/Examiner:	Title, Name-Surname (Institution)	(Signature)
Member/Examiner:	Title, Name-Surname (Institution)	(Signature)
Member/Examiner:	Title, Name-Surname (Institution)	(Signature)

APPROVAL

This thesis has been deemed by the jury in accordance with the relevant articles of Yeditepe University Graduate Education and Examinations Regulation and has been approved by Administrative Board of Institute with decision dated …….. and numbered .....

(Signature)

Prof. Dr. Bayram Yılmaz

Director of Institute of Health Sciences

DECLARATION

I hereby declare that this thesis is my own work and that, to the best of my knowledge and belief, it contains no material previously published or written by another person nor material which has been accepted for the award of any other degree except where due acknowledgment has been made in the text.

15.05.2022

Rabia Sena Türker

ACKNOWLEDGEMENTS

I would like to express my gratitude to my supervisor Professor Bayram Yılmaz and my co-supervisor Associate Professor Dr. Ramazan Üstün for the guidance and support, Associate Professor Burcu Gemici Başol for her important contributions with the statistical analyses, Associate Professor Yıldıray Başbuğan and technician Orhan Aslan for providing the best cooperation at the YUDETAM. Also, my deepest respects and admirations to my father for being an inspiration since the moment I opened my eyes to this world, my mother and sister for their moral support, and my dear friend Ceren Yener for always amplifying my motivation whenever I needed.

This study would not be completed without the support of Van Yüzüncü Yıl University Scientific Research Projects Department, I would like to thank to this department for the financial support.

TABLE OF CONTENTS

LIST OF TABLES

LIST OF FIGURES

LIST OF SYMBOLS AND ABBREVIATIONS

10-HDA	10-hydroxy-2-decenoic acid
ACh	Acetylcholine
BDNF	Brain Derived Neurotrophic Factor
BNG	Bungarotoxin
CNS	Central Nervous System
CNTF	Ciliary Neurotrophic Factor
DRG	Dorsal Root Ganglion
EGM	Turkish General Directorate of Security
ERR	Estrogen Related Receptor
FGF	Fibroblast Growth Factor
GDNF	Glial Cell-line Derived Neurotrophic Factor
GF	Growth Factor
HLRWT	Horizontal Ladder Rung Walking Test
IGF	Insulin-like Growth Factor
IL	Interleukin
LIF	Leukemia Inhibitory Factor
LTP	Long Term Potentiation
MAPK	Mitogen-Activated Protein Kinase
MEGF	Mouse Epidermal Growth Factor
NAR	Nicotinic Acetylcholine Receptor
NCAM	Neural Cell Adhesion Molecule
NFAT	Nuclear Factor of Activated T-cells
NF	Neurotrophic Factor
NFH	Neurofilament Heavy Chain
NF-κB	Nuclear Factor Kappa B
NGF	Neuron Growth Factor
NT	Neurotrophin
P0	Myelin Protein Zero
P75NTR	P75 Neurotrophin Receptor
PDGF	Platelet Derived Growth Factor
PI3K	Phosophoinositide 3-kinase

PLC	Phospholipase C
PNI	Peripheral Nerve Injury
ProBDNF	BDNF Precursor
ProNGF	NGF Precursor
PNS	Peripheral Nervous System
RJ	Royal Jelly
SC	Schwann Cell
SGK	Social Security Institution of Turkey
STAT	Signal Transducer and Activator of Transcription
TAM	Tumor Associated Macrophage
TGF-β	Transforming Growth Factor Beta
TNF-α	Tumor Necrosis Factor Alpha
TNFR	TNF Receptor
TrkA	Tropomyosin Receptor Kinase A
TrkB	Tropomyosin Receptor Kinase B
WD	Wallerian Degeneration

ABSTRACT

Türker, R. S. (2022). The Morphological and Functional Evaluation Of 10-Hydroxy-2-Decenoic Acid's Regenerative Effect on Mouse Sciatic Nerve Crush Model. Yeditepe University, Institute of Health Sciences, Doctoral Program in Neuroscience, PhD Thesis, İstanbul.

Traumatic injury of peripheral nerves results in loss of motor and sensory functions. It seriously weakens the workforce and decreases the quality of life. 10-hydroxy-2-decenoic acid (10-HDA) is the predominant fatty acid of royal jelly which is known for its neuroprotective effects. We hypothesize that 10-HDA may accelerate regeneration and recovery after crush injury. The 40 mice were randomly assigned to sham group, sciatic nerve crush group, HDA 30 treatment group, and HDA 60 treatment group. The mice (except sham group) were exposed to sciatic nerve crush injury. One hour after injury, the mice were given 0.9% saline solution or 10-HDA (30 and 60 mg/kg) orally through flexible gavage daily for 4 weeks. The functional recovery was evaluated using thermal hyperalgesia, sciatic function index, rotarod, electromyography, and horizontal ladder rung walking tests. Microstructural changes of the crushed sciatic nerve were analyzed using the ImageJ software for immunofluorescence images of neurofilament (NFH), βIII-tubulin (βIII), myelin protein zero (P0), nicotinic acetylcholine receptor (NAR), and S100 protein on the longitudinal section of the sciatic nerve. We observed that 10-HDA significantly recovered motor and sensory functions at two weeks post-injury. Laser scanning confocal microscopy demonstrated that 10-HDA significantly increased regeneration of NFH, βIII, P0, NAR, S100 structures. Especially the 30 mg/kg dosage of 10-HDA showed promising results. In conclusion, 10-HDA has shown to possess a strong therapeutic effect on sciatic nerve crush injury, which is one of the most common models of peripheral nerve injury in mice.

Keywords: Peripheral Nerve Injury, 10-Hydroxy-2-Decenoic Acid, Immunohistochemistry, Functional Recovery, Regeneration, In vivo

The study was supported by Van Yüzüncü Yıl University Scientific Research Projects Department Project No TDK-2021-9481.

ABSTRACT (Turkish)

Türker, R. S. (2022). Siyatik Sinir Crush Hasarı Oluşturulmuş Farelerde 10-hidroksi-2-dekenoik Asidin Rejeneratif Etkisinin Morfolojik ve Fonksiyonel Olarak Değerlendirilmesi. Yeditepe Üniversitesi Sağlık Bilimleri Enstitüsü, Sinirbilim Doktora Programı, Doktora Tezi. İstanbul.

Periferik sinirlerin travmatik hasarı, motor ve duysal fonksiyonların kaybına neden olur. Bu durum iş gücünü ciddi anlamda zayıflatır ve yaşam kalitesini düşürür. 10-hidroksi-2-dekenoik asit (10-HDA), nöroprotektif etkileri ile bilinen arı sütünün baskın yağ asididir. Bu çalışmada 10-HDA'nın ezilme hasarından sonra sinir rejenerasyonunu ve fonksiyonel iyileşmeyi hızlandırdığı hipotezi araştırılmıştır. 40 adet fare rastgele sham grubuna, siyatik sinir ezilme grubuna, HDA 30 tedavi grubuna ve HDA 60 tedavi grubuna ayrıldı. Fareler (sham grubu hariç) siyatik sinir ezilme hasarına maruz bırakıldı. Yaralanmadan bir saat sonra, farelere 4 hafta boyunca günlük olarak esnek gavajla oral yolla %0.9 salin veya 10-HDA (30 ve 60 mg/kg) verildi. Fonksiyonel iyileşme termal hiperaljezi, siyatik fonksiyon indeksi, rotarod, elektromiyografi ve yatay merdiven basamak yürüme testleri kullanılarak değerlendirildi. Ezilmiş siyatik sinirin mikroyapısal değişiklikleri, nörofilament (NFH), βIII-tubulin (βIII), miyelin protein sıfır (P0), nikotinik asetilkolin reseptörü (NAR) ve S100 proteininin immünofloresan görüntüleri ImageJ yazılımı kullanılarak analiz edildi. Yaralanmadan iki hafta sonra 10-HDA'nın motor ve duyusal fonksiyonları önemli ölçüde iyileştirdiği gözlendi. Lazer taramalı konfokal mikroskopi görüntüleri, siyatik sinir kesitleri üzerinde 10-HDA'nın NFH, βIII, P0, NAR ve S100 yapılarının rejenerasyonunu önemli ölçüde arttırdığını gösterdi. Özellikle 30 mg/kg 10-HDA dozu umut verici sonuçlar ortaya koydu. Sonuç olarak, 10-HDA'nın farelerde periferik sinir hasarının en yaygın modellerinden biri olan siyatik sinir ezilme hasarı üzerinde güçlü bir terapötik etkiye sahip olduğu gösterildi.

Anahtar Kelimeler: Periferik Sinir Hasarı, 10-Hidroksi-2-Dekenoik Asit, Immünohistokimya, Fonksiyonel İyileşme, Rejenerasyon, İn vivo

Bu çalışma Van Yüzüncü Yıl Üniversitesi Bilimsel Araştırma Projeleri Koordinasyon Birimi tarafından TDK-2021-9481 numaralı proje ile desteklenmiştir.

1. INTRODUCTION AND PURPOSE

Unlike the central nervous system (CNS), which is protected by the skull and vertebrae, the peripheral nervous system (PNS) is not protected by bones, therefore it is more susceptible to trauma. Peripheral nerve injuries (PNI) are a common health problem in clinics worldwide. It seriously weakens the workforce also decreases the quality of life. Lesions are mostly caused by motor vehicle accidents, work accidents, penetrating injuries, gunshot injuries, ischemia and crush trauma. Today, motor vehicle accidents are the most responsible of PNI etiology. According to the data obtained from the statistics of the Turkish General Directorate of Security (EGM), 183,710 traffic accidents occurred in Turkey in 2018, and 310,109 people were injured in these accidents [1].

According to the statistics of the Social Security Institution of Turkey, 359,653 occupational accidents occurred in our country in 2017, and 47.73% of the employees received an incapacity report for at least 1 day as a result of the accidents [2].

PNI occurs in 2.8% of multiple trauma cases. In the United States, the prevalence of traumatic peripheral nerve injury in level I trauma centers is approximately 2.8%. PNI can affect all age groups, including children and adults, depending on etiological reasons [3–7].

PNI causes permanent disfunctions. Painful neuropathies that cause paralysis and muscle weakness, loss of sensation and autonomic dysfunctions occur due to damage to the nerve and the muscles it innervates. Long denervation time worsens the muscle atrophy and leads to a contracture development. Severe neurological damage occurs in PNI resulting from gunshot wounds. In summary, severe nerve injury has a devastating effect on the patient's quality of life [3,7–10].

In PNI, following the interruption of the axonal integrity; phenotypic changes occur in damaged neurons and other cells. Inflammation pathways of sensory and motor neurons are triggered, Wallerian degeneration begins in the distal segment of the injured axon between the 24th and 48th hours, targeting the removal of myelin sheath and cellular debris [8,11]. In the proximal segment of the axon, the destruction process continues until the last intact node of Ranvier. Anterograde Schwann cells (SC) begin to catabolize the myelin sheath. Tissue macrophages also phagocytose the remnants so that the myelin sheath is completely destroyed. During this time, the injury signals are carried retrogradely towards the soma [11–14].

Numerous conservative, medical and surgical approaches have been described for the treatment of peripheral nerve injuries. With the understanding of the pathophysiology of PNI, many agents and modalities that are thought to increase regeneration by acting at certain stages

of the healing process have been tried and tested. Although there is currently no agent that can be the gold standard apart from the conservative and surgical approach in different types of injury, many agents have been found to have positive and promising contributions to nerve healing. Modalities and agents whose contributions to peripheral nerve healing have been investigated include exercise, electrical stimulation, magnetic field induction, synthetic and natural polymers, antioxidants, neurotrophic factors, immune-modulators, stem cells, and many more [8,15,16].

Experimental treatments designed to increase the rate of axonal regeneration by stimulating Schwann cells in distal nerve segments can overcome nerve transection, form a myelin sheath around regenerating axons, and thereby achieve clinically significant functional improvement [17]. Although peripheral nerve fibers show significant potential for self-regeneration, the result is often unsatisfactory. This mechanism results in poor motor recovery and irreversible sensory dysfunction [9]. The healing process of PNI and its re-innervation to the targeted tissue are multifactorial and complex processes involving different cells, growth factors and signaling pathways. For this reason, the correct restructuring of the nerve tissue and neuromuscular junction and recovery at a functionally acceptable level continue as a clinical problem in PNI. Despite recent advances in treatment strategies, PNI remains one of the most important health problems with its increasing incidence worldwide. Today's treatment approaches do not provide a full recovery and also contain many disadvantages [7].

Royal jelly (Royal Jelly-RJ) is a thick and milky secretion synthesized in the hypopharyngeal and mandibular glands of young worker bees (*Apis mellifera* L.) [18]. While the queen honey bee feeds on this milk during the larval stage, worker honey bees are fed for only 3 days. That's why RJ is associated with longer life expectancy of queen bees. RJ is an important functional food ingredient with many health promoting properties. RJ is considered a multi-nutrient source, its composition includes water, proteins, carbohydrates, lipids, vitamins, minerals, acetylcholine and other bioactive substances. The high nutritional value of RJ is due to the unique combination of all the nutrients and body-building ingredients it contains. Today, it is used for health purposes in many sectors from the pharmaceutical and food industries to the cosmetics and manufacturing sectors in different parts of the world [18]. It is one of the most sought-after functional products as a commercial commodity, especially in dietetics and cosmetics. In animal models, RJ has been shown to have numerous functional properties such as anti-aging, stomach and liver protective, anti-inflammatory, anti-oxidant, antibacterial, vasodilodative, hypotensive, disinfectant, hypoglycemic, antihypercholesterolemic and antitumor properties [19]. It has been reported to alleviate neuronal apoptosis, reduce amyloid

plaque pathology, and improve behavioral disorders in Alzheimer's model. It has also been reported to reduce anxiety, increase energy, promote growth, improve memory, and have neuromodulatory and neuroprotective effects [20]. The biological activities of RJ are mainly attributed to bioactive fatty acids, proteins and phenolic compounds [21].

Queen bee acid (10-hydroxy-2-decenoic acid, 10-HDA) is the predominant fatty acid of royal jelly [18]. 10-HDA constitutes approximately 5% of the active content of RJ and 40% of the total fatty acids. The freeze-dried RJ composition contains 8–19% lipid. Most of the lipids are made up of 10-HDA in RJ. 10-HDA has been accepted as the most important compound of RJ in the international standards quality assessment and has been reported to be responsible for important biological activities [18]. 10-HDA has activity on estrogen receptors that affect brain function and body composition [19]. In an experimental chronic stress model, intraperitoneal treatment of mice with 10-HDA decreased anxiety and depression-like behaviors and increased body weight [19]. On the other hand, 10-HDA administration inhibited glia proliferation and promoted the stimulation of neuritogenesis from stem cells in vitro. Moreover, it increased the neurite outgrowth of primary hippocampal neurons, significantly reduced hypoxia-induced neuron death, and significantly increased mitochondrial health in vitro. The results show that 10-HDA has therapeutic effects on brain health during normal development and aging, and may combat age and stress-related weight loss [22].

The aim of the present study was to investigate the regenerative effects of 10-HDA and elucidate underlying mechanisms in regeneration process.

The importance of the thesis:

This is the first study based on the regenerative effects of 10-HDA on sciatic nerve crush model. According to the results, 10-HDA has been found very effective on peripheral nerve regeneration which might be a treatment option for patients with PNI.

This thesis is about unrevealing beneficial effects of a novel molecule which might be used as a potential therapeutic agent.

Research hypothesis:

10-HDA has a regenerative effect on mice sciatic nerve injury.

2. LITERATURE REVIEW

2.1. Peripheral Nerve Injury

The nervous system is divided into two main parts, central and peripheral nervous system. Central nervous system (CNS) includes cerebrum (brain), cerebellum, brainstem, medulla spinalis and the first and second cranial nerve [23]. Peripheral nervous system (PNS) includes the 3rd to the 12th cranial nerves and their branches which innervate the muscles and organs.

Lesions mostly occur with motor vehicle accidents, work accidents, penetrating injuries, gunshot injuries, ischemia and crush trauma [6].

The regeneration capacity of both systems is drastically different. Peripheral nerves have a high regeneration capability while central nervous system neurons do not [24].

A peripheral nerve has three different layers. These are epinerium, endonerium and perinerium.

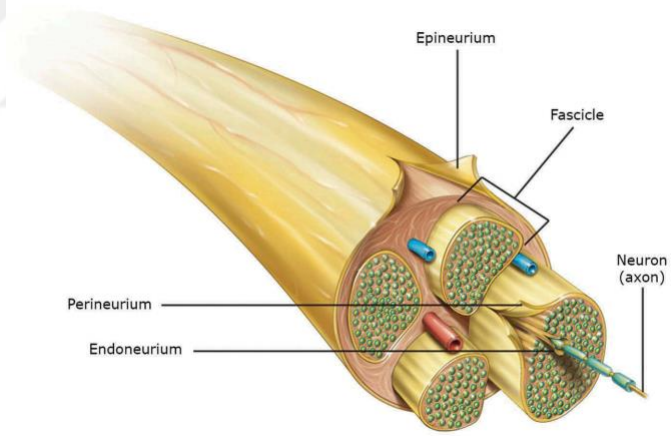

Figure 2.1. The layers of a peripheral nerve [25].

2.1.1. Definition

The definition of PNI has been changed over time. It was first classified at 1943 by Seddon and then refined by Sunderland at 1951 [25]. The recent classification table includes both the injury definition and recovery potential. There are 5 stages of degeneration which starts with Type 1, focal demyelination; followed by Type 2 which includes the damage to the axon which endoneurium, perineurium and epineurium are intact; Type 3 a damage to the axon and endoneurium and the rest is intact, Type 4 damage to axons, endoneurium and perineurium

however epineurium is intact, finally ends with Type 5 the complete loss of continuity [25].

Seddon	Sunderland	Injury	Recovery potential
Neuropraxia	Type 1	Focal demyelination	Full (1 day to 3 months)
	Type 2	Damage to axons; endoneurium, perineurium, and epineurium intact	Full (2 to 4 months)
Axonotmesis	Type 3	Damage to axons and endoneurium; perineurium, and epineurium intact	Partial (12 months)
	Type 4	Damage to axons, endoneurium, and perineurium; epineurium intact	Surgery is required for recovery
Neurotmesis	Type 5	Complete loss of continuity	Surgery is required for recovery

Figure 2.2. Classification of the peripheral nerve injury types [25].

2.1.2. Peripheral Nerve

Peripheral nervous system (PNS) is consisted of sensory and motor divisions. The motor division is consisted of autonomic and somatic subdivisions.

While the afferent sensory fibers of the PNS convey sensory information from sensory receptors to regions of the brain, the efferent motor fibers deliver nerve impulses away from the CNS to the target organs like glands or muscles via the neuromuscular junction. Hence, the PNS plays an important role of mediating the relationship between the organism and the environment. The bodies of sensory spinal nerves are embedded in the dorsal part of the spinal cord, although the motor spinal nerves' body is located in the anterior part of the spinal cord. The impulse enters the spinal cord from the dorsal horn and leaves it from the anterior horn. There might be an interneuron which modulates the information [23].

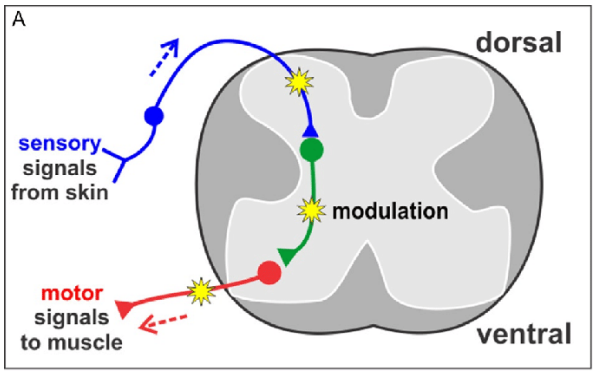

Fig 2.3. The dorsal and anterior organization scheme of the spinal cord [26].

The primary efferent fibers are classified in 4 groups according to their diameter. They also have different functions as seen in the figure below.

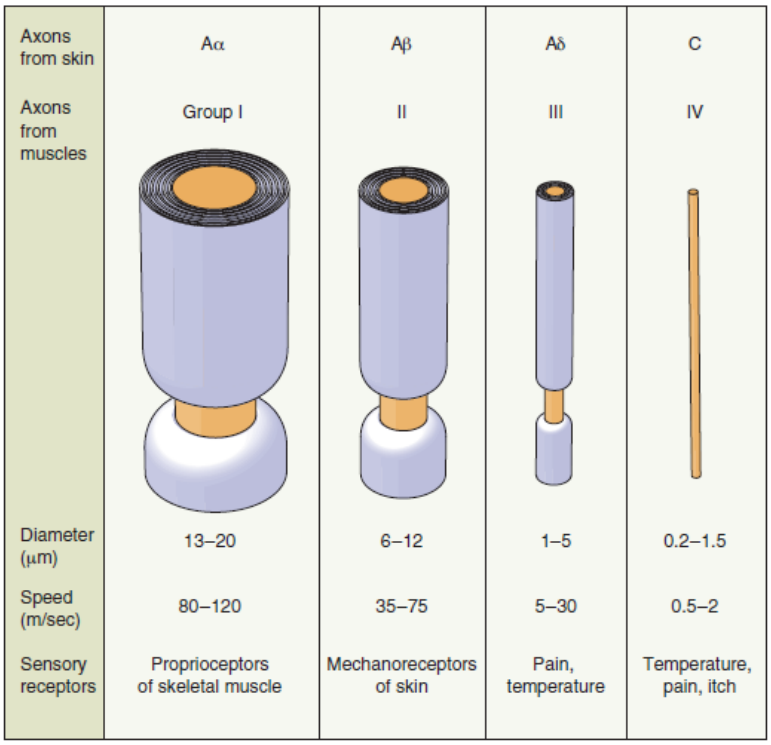

Fig 2.4. The classification of the primary efferent fibers [27].

The autonomic division of the PNS works under voluntary control and the somatic division involuntarily regulates the homeostasis of internal organs [23].

2.1.2.1. Neuromuscular Junction

The NMJ (Neuromuscular Junction) is formed where the motor neurons innervate the skeletal muscle fibers which are wrapped by the Schwann cells [28]. It is a typical electrochemical synapse controlled by the neurotransmitter Acetylcholine (ACh). The action potential arrives to the end of the motor neuron and activates the ACh release from the nerve terminal. The ACh in the synaptic cleft binds to the nicotinic ACh receptors (NAR) which are located on the muscle fibers and causes a depolarization on the muscle cell, triggers calcium release from the sarcoplastic reticulum in order to initiate muscle contraction. The malfunction of this process causes serious motor function deficits like Myasthenia Gravis or Congenital Myasthenic Syndrome [28].

2.1.2.2. Dorsal Root Ganglion

The Dorsal Root Ganglion (DRG) is found in every level of the spinal cord and has a bilateral formation which is housed in a fixed vertebral structure (neuroforamen) spanning the information from the spinal cord and peripheral vertebral column. It mostly consists of the neural bodies. One single DRG might shelter up to 15000 neurons with a 20 to 150 μm diameter. These neurons usually convey information from different types of modalities such as nociceptive information (temperature, mechanical, and chemical-induced) or peripheral sensation. The DRG neurons also play a crucial role on pain modulation [29].

2.1.3. History

According to the very early reports, the physicians had no information about the difference between tendons and nerves. It appears to be clarified at Alexandrian age first, by the Alexandrian school [30].

The first peripheral nerve surgery records belong to the 7th century, Paul of Aegina, which describes the handling methods of tissue and little information about suturing [31]. Within the beginning of 19th century, the wars and their expected consequences resulted with a tremendous development of examination and operation techniques for nerves. Here is a drawing showing the techniques of leading physicians of the century.

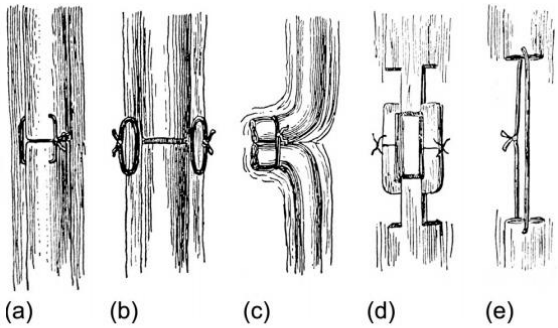

FIGURE 2.3 Nineteenth-century direct suture techniques. (a, b) Perineurotic suture; (c) Rawa's co-apted suture; (d) Létiévant's nerve flap technique; (e) Suture à la distance.

Figure 2.5. The outstanding techniques of 19th century physicians; Perineurotic suture (a, b), Rawa's cadapted suture (c), Letievant's flap technique (d), Suture a la distance (e) [32].

The 20th century, George Woolsey recommended a new technique that suggested the injured nerves to be wrapped with a Cargile membrane produced from ox peritoneum in order to prevent the adhesions [32]. William Wayne Babcock used the first nerve clamp to transfix the nerve ends in 1927. The first nerve graft was mentioned in 1956 at an article. At 1988, the first

biodegradable polyglycolic acid tubes were usen by Dellon and Mackinnon [32].

2.1.4. Etiology

The major causes for the PNI are motor vehicle accidents and gunshot wounds. The following causes might be sharp and penetrative objects, burning wounds, radiotherapy, iatrogenic operational problems (injections, prosthesis, tumor excisions, intravenous catheterization etc.) [33]. In addition, compression injuries such as carpal and cubital tunnel and crush injuries are some other causes at the PNI etiology [34]. Finally intraneural fibrosis is an intrinsic cause of a PNI [35].

2.1.5. Pathophysiology

Following the injury, the pathophysiological alterations start in seconds. Depending on the severity of the damage, the neuron decides to regenerate itself or rather terminate its life by apoptotic pathways. The myelin disintegration, varicose swelling, axonal contour impairment, neurotubule and neurofilament degeneration are the main steps of the degeneration [36]. This specific process has been named after Augustus Waller at 1850 after his definitive study based on nerve injury mechanisms [37].

2.1.5.1. Wallerian Degeneration

Augustus Waller, the first scientist to explain this phenomenon studied with the frog glossopharyngeal and hypoglossal nerves [37]. During his examination after axotomy, he realized the nerve parts were getting distant and “spongy”. He also observed the disappearance of the myelin sheath and turning into fusiform masses. After a half century, Cajal affirmed and detailed the study with a very comprehensive histological description by also proving the leukocyte infiltration [37].

Wallerian degeneration (WD) precisely describes the biological process following the neuron degeneration. The first 24-48 hours is the degeneration and disintegration of the axolemma and axoplasm which is followed by the calcium influx and prompt axonal breakdown via the proteases in charge. The Schwann cells start to dedifferentiate, and the synthesis of the myelin proteins are downregulated. The myelin debris forms the bands of Büngner which form the tubes that guides the regenerating fibers. A following release of cytokines, adhesion molecules and neurotrophic factors is the last stage of WD [38,39].

2.1.5.2. Phagocytosis

Phagocytosis is a phenomenon explaining the disposal of pathogens, apoptotic cells, or particles by phagocytes. It is the main key of cellular immunity and works through the recognition and ingestion of particles bigger than 0.5 μm into a phagosome which is a membrane vesicle [40].

The main cell type in the PNS which is responsible from this process is Schwann cells which cover the peripheral nerves and attribute to the myelin sheath [41]. The effective clearance of the debris is crucial for a successful regeneration since myelin is a roadblock for recovery in the PNS [42]. The resident macrophages in the epineurium also take part at this process. It has been shown that SC's have 2 types of phagocytic receptors; TAM receptors (Axl-, Mertk-, and Tyro3-) and MEGF10 (multiple EGF-like-domains-10) which are upregulated post injury [43].

2.1.6. Regeneration Mechanisms

There is a considerable number of proteins, factors, receptors, and pathways taking role in the peripheral nerve regeneration process. Axon guidance has a key role at this sensitive repair mechanism. Also there is a critical time window for the axon to reach the target since the target tissue might lose its receptive answer for reinnervation [44].

The first step requires a retrograde injury signal transmission to the soma via importin proteins [45,46]. The distal stump of the injured nerve goes through a differentiation. The Schwann cells attached to the axon start to down-regulate their myelin expression levels and rather start up-regulating the expression of growth factors and cell adhesion molecules [24]. If the regeneration process is tending to fail, retraction bulbs appear. Vice versa, growth cones which include actin fibers are an indicator for a successful regeneration [47].

2.1.6.1. Growth Cones

Ramón y Cajal was the first to name this physiological structure that is the first step of regeneration. It is found both in the axon and the dendrite and they basically guide the neuron with positive or negative feedback and regulate the cytoskeleton structure. A growth cone has three major compartments. The central core is rich with mitochondria and microtubules whereas the filopodia and lamellipodia have a very low intensity of mitochondria. The motile, actin-rich minor slender extensions called filopodia make projections from the growth cone and sense environmental signals. The ruffled look between the filopodia is called lamellipodia which are also motile [48].

The studies over growth cones showed that a PNS neuron can grow a growth cone within hours following an axotomy [49]. The first trigger of the production of a growth cone is Calcium influx. After an injury, the membrane integrity is disrupted and therefore the extracellular Calcium rushes into the neuron through the gaps [50]. Some studies showed that the regeneration in a Calcium-free environment doesn't succeed because of the growth cone production failure [51]. This Calcium influx leads to the "sealing patch" production which helps regaining the membrane integrity [52]. Following the retrograde microtubule depolymerization wave along an axonal segment, in parallel, actin molecules in the adhesion complexes depolymerize [53]. The depolymerization helps the plasma membrane to disengage from its surroundings and gives mechanical freedom to axonal membrane to collapse which leads to assemble the growth cone structure [54].

Integrins and IgCAMs which are adhesion proteins from the immunoglobulin superfamily or extracellular matrix proteins like laminins, fibronectins and thrombospondins mediate the axon-growth cones anchoring and elicit cytoskeletal responses [55]. Besides, a strong adhesion provided by N-cadherin and integrins (NCAM), translates the myosin-driven actin filaments flow into growth cone movement that attenuates the retrograde flow, enhances the actomyosin mediated traction force and pulls the growth cone forward [56]. Likewise, there are so many molecules and receptors that have been proven to be regulating the axon growth through the growth cone such as; neurotropic proteins Slit, DCC, FAK, Src, Fyn, adhesion proteins integrins, L1 with Plexins, neuropilins which are components of the receptor complexes of semaphorins etc. [57–63].

2.1.6.2. Neurotrophic Factors

Neurotrophic factors (NFs) are polypeptide molecules which support cell survival, differentiation, proliferation, and morphogenesis in the peripheral nerve system of mammalians [64]. These constructive effects mostly function through intrinsic transduction potentials and molecular/mechanical signaling regulations after receptor-mediated processes [65].

There are four main Neurotrophins (NTs) are: neuron growth factor (NGF), brain derived neurotrophic factor (BDNF), neurotrophin-3 and 4 (NT-3 & NT-4). Other classes of proteins include transforming growth factor-β (TGF-β) family, the interleukin-6 related cytokines (IL-6) and fibroblast growth factors (FGFs). The glial cell line derived neurotrophic factor (GDNF) family provide the survival of sensory and sympathetic neurons [48].

The growth factor (GF) members; fibroblast growth factors (FGFs) and nerve growth factor (NGF) are secreted by SCs or neurons. In the PNS, GFs provide the regenerating

microenvironment of axonal sprouting and elongation after nerve injury [66].

Growth Factors:

NGF: The sequences of this neurotrophin have been showed that it is a highly protected molecule, sharing important homology within different species [67]. The mature and active form of NGF is descended from ProNGF, which also has crucial roles during development and adulthood, having either neurotrophic and pro-apoptotic properties [68].

NGF exerts its biological activity by the tropomyosin kinase receptor A (TrkA) [69]. The major pathways regulated by the TrkA are phosphatidylinositol-3-kinase (PI3K)-Akt, extracellular signal-regulated kinase (ERK), Ras-mitogen activated protein kinase (MAPK), and Phospholipase C (PLC)-γ [70]. NGF also activates the non-selective, low-affinity, transmembrane glycoprotein p75 pan-neurotrophin receptor (p75NTR) by binding. It regulates signaling via TrkA [71]. The NGF - p75NTR binding activates additional signaling pathways. In the lack of co-expressed TrkA, might lead a signal that causes a cell to die via apoptosis [72]. Signaling pathways controlled by p75NTR are the NF-κB, Jun kinase signaling cascade, and ceramide generation [73].

FGF: FGFs have been proven to enhance the survival and neurite extension of neurons as well as neuronal functions and wound healing [74]. A subtype FGF2 is present at the blood-brain barrier and its production is provided by astrocytes, also has effects on astrocyte proliferation [75]. FGF-2 expressions increase after injury at the distal and the proximal stumps of the nerve. It also supports fiber outgrowth, branching, vascularization, proliferation, myelination; also prevents the lesion induced neuronal death and apoptosis. While FGF-3 is related to cell death, FGF-1 and 2 are related to cell survival [76]. FGF-1 receptors use Ras-dependent pathways whereas FGF-3 receptors use a Ras-independent pathway [77].

IGF: Insulin like growth factor (IGF) acts on both neurons and denervated muscles to inhibit denervation-induced atrophy. It has a 5 minute short half-life [78]. The anti-apoptotic and positive trophic effects of IGF-1 are mediated via the MAP-kinase and PI3K-Akt pathways [79].

PDGF: Platelet-derived growth factor (PDGF) is produced by Schwann cells. PDGF family has 4 known families as PDGF-A, B, C and D. Both PDGF and receptors are expressed in SCs. PDGF-B acts as an autocrine mitogen, prevents the apoptosis of Schwann cells and hence is a survival factor for these cells [80]. These activities are provided in synergy with NT-3 and IGF [81].

Trophic Factors:

The most known trophic factors are NT-3 & 4, BDNF, CNTF and GDNF.

NT-3: NT-3 was firstly found to support the chick trigeminal mesencephalic neurons' survival [82]. It is known that NT-3 has a crucial role as a trophic factor for the sympathetic and sensory neuron growth [83]. Since it can bind to TrkA, TrkB and p75NTR receptors with a low affinity, NT-3 is a remarkably indiscriminate NT member. Besides, it binds to TrkC with the highest affinity [84]. NT-3 also prevents peripheral sensory axons' degeneration and improves functional response in them [85].

NT-4: NT-4 regulates the neuronal network development via providing the growth of neuronal processes, plasticity and synaptic development, differentiation and neuronal survival [86]. According to a study, the expression of NT-4 reduces during the injury, however 2 weeks post-injury, the NT-4 mRNA level is upregulated in the distal stump of the injured sciatic nerve [87]. Moreover, NT-4 application to rat sciatic nerves resulted in enhanced axon regeneration, increased the number of regenerated axons, myelin thickness and axonal diameter [88].

BDNF: Brain derived neurotrophic factor is involved in the CNS functions such as long-term potentiation (LTP), synaptic plasticity, learning and memory, also post-injury neurogenesis and regeneration [89]. BDNF can bind to two receptors, tropomyosin receptor kinase B (TrkB) or p75NTR. BDNF preferentially binds TrkB, ensuing in pro-growth signaling, however proBDNF preferentially binds p75NTR, causing in antigrowth signaling [90]. BDNF is mainly secreted as proBDNF [91].

CNTF: Ciliary neurotrophic factor supports the differentiation and survival of neurons during development. The CNTF receptor has 2 components; CNTFRα is present in nerve and muscle, and LIFRβ/gp130 heterodimer is localized in nerve and macrophages. CNTF-like activity was demonstrated in sciatic, hypoglossal, and sural nerves and is mostly immunolocalized to larger myelinated fibers' Schwann cells. It has a trauma-dependent release of the protein from Schwann cells via retrograde axonal transport of itself after nerve injury. There is also growing evidence that CNTF may be contributing to maintenance of uninjured neurons, and the ability of neurofilament synthesis [92].

GDNF: Schwann cells express GDNF mRNA in peripheral nerves. As a response to a nerve transection, GDNF mRNA expression in sciatic nerves and Schwann cells rises dramatically [93]. It was firstly found to provide the differentiation and survival of dopaminergic neurons via supporting dopamine uptake from cultured rat glial cells [94].

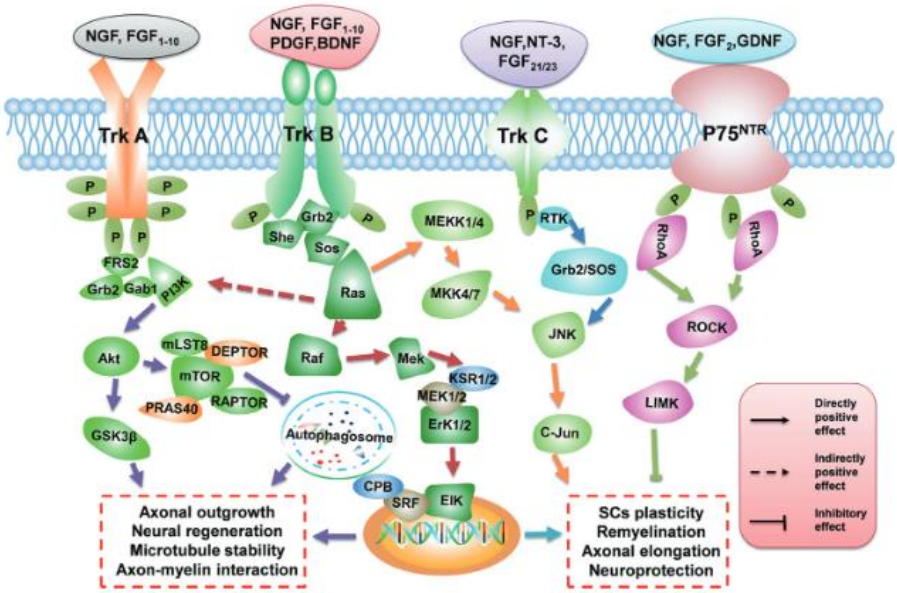

Fig. 2.6. Neurotropic factors and their mechanism of action [9].

2.1.6.3. Cytokines

TNF-α: The pro-inflammatory cytokine Tumor necrosis factor-α coordinates and regulates the immune response following the injury via initiating the activation of cytokine and growth factors' cascade [95]. It has two receptors which are TNF-R1 and the low affinity TNF-R2. They both can be expressed from the neurons and glia. While TNF-R1 is responsible from neuronal death, TNF-R2 regulates neuroprotection and proliferation due to its T-cell relation. The SC's and macrophages release TNF-α leading to an extensive recruitment of macrophages again. It has also been reported that TNF-α has following roles such as promoting the blood-nerve barrier degradation, demyelination, reorganizing endoneurial space, remodeling the extra-cellular matrix, and decreasing SC proliferation [95–99].

TGF-β: Almost every cell in the body produces TGF-β including endothelial, hematopoietic, neuronal, epithelial, and connective tissue cells. It has 3 well-known receptors as type-I, II and III. One subtype TGF-β1 was shown to be a signaling molecule that mediates the normal growth and development. It is being produced by SCs, having a mitogen activity, and increasing premyelination markers, and adhesion molecules. TGF-β1's proliferatic movement is strengthened following the injury, and it is downregulated once the fibers are grown back to the distal stump, allowing a proper ensheathment and myelination [100,101].

LIF: Leukemia inhibitory factor is a neuropoietic cytokine in the nervous system involved in the general response to trauma. It governs the sympathetic neurons' cholinergic switch and enhances the survival and differentiation of sympathetic neurons. It is known that

the mRNA expression of LIF is rapidly increasing at the SCs during injury; the rapid and local release of LIF is followed by the uptake and retrograde transport by the neurons. It has also been shown that LIF is associated with the sprouting of DRG neuron fibers following axotomy [102]. The expression of the LIF gene is regulated by a large number of factors, including transcription factor 2, c-Myc transcription factor, JUN gene (c-Jun), a transcription factor ETS (Erythroblast transformation specific), Max, NFAT, p53, STAT1-β, STAT2, and STAT5A, and potentially other factors. It is strongly involved in the MAPK pathway. There is also a synergistic mechanism between LIF and other factors, LIF induces the IL-1 β expression and forms a positive feedback loop [103]. The same relationship is established with epidermal growth factor LIF and TGF- β [104].

IL-6: Interleukin-6 is a glycoprotein with a pro-inflammatory activity which enhances T-cell activation and works as a neurotrophic factor. It has a massive role in neuroprotection and pain modulation via activating the JAK/STAT pathway. It can also directly modulate neuronal activity by causing the release of neuropeptide transmitters, increase the expression of RAGs (Regeneration associated genes), and promote neurite outgrowth. IL-6 production from the fibroblasts is induced by IL-1 and TNF-α, which are also produced by SCs. It has been found that the IL-6 receptor subunit IL-6Rα was also upregulated after injury at the DRG (Dorsal Root Ganglion) neurons [105–108].

2.2. Royal Jelly

Royal jelly (RJ) is a thick and milky secretion synthesized in young worker bees' hypopharyngeal and mandibular glands (*Apis mellifera* L.) [18]. While the queen honeybee is fed with this milk during the larval stage, worker honeybees are fed for only three days. That is why RJ is associated with a longer life expectancy of queen bees [18]. RJ is an essential functional food ingredient with many health promoting properties. It is considered as a multi-nutrient source; its composition includes water, proteins, carbohydrates, lipids, vitamins, minerals, acetylcholine and other bioactive substances. The high nutritional value of RJ is due to the unique combination of all the nutrients and body-building ingredients it contains. Today, it is used for health purposes in many sectors, from the pharmaceutical and food industries to the cosmetics and manufacturing sectors in different parts of the world. It is one of the most sought-after functional products as a commercial commodity, especially in dietetics and cosmetics [18,19,109].

2.2.1. Pharmacological Effects

In animal models, RJ has been shown to have numerous functional properties such as anti-aging, stomach and liver protective, anti-inflammatory, antioxidant, antibacterial, vasodilatative, hypotensive, disinfectant, hypoglycemic, antihypercholesterolemic, and antitumor properties [19]. It has been reported to alleviate neuronal apoptosis, reduce amyloid plaque pathology, and improve behavioral disorders in Alzheimer's model [21]. It has also been reported to reduce anxiety, increase energy, promote growth, improve memory, and have neuromodulatory and neuroprotective effects. The biological activities of RJ are mainly attributed to bioactive fatty acids, proteins, and phenolic compounds [19,109].

2.3. 10-HDA

Queen bee acid (10-hydroxy-2-decenoic acid, 10-HDA) is the predominant fatty acid of royal jelly. 10-HDA constitutes approximately 5% of the active content of RJ and 40% of the total fatty acids. The freeze-dried RJ composition contains 8–19% lipid. Most of the lipid is made up of 10-HDA. 10-HDA has been accepted as the most crucial compound of RJ in the international standards quality evaluation and has been reported to be responsible for important biological activities [18,19].

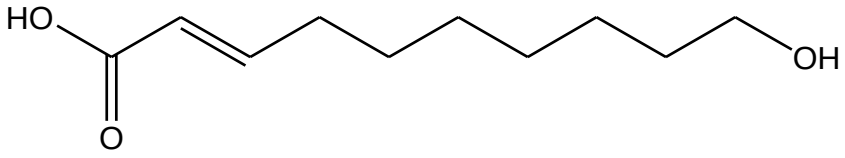

Fig 2.7. Chemical structure of 10-hydroxy-2-decenoic acid

2.3.1. Pharmacological Effects

10-HDA has activity on estrogen receptors that affect brain function and body composition. In an experimental chronic stress model, intraperitoneal treatment of mice with 10-HDA decreased anxiety and depression-like behaviors and increased body weight [110]. On the other hand, 10-HDA administration inhibited glial proliferation and promoted the stimulation of neuritogenesis from stem cells in vitro. It increased the neurite outgrowth of primary hippocampal neurons, significantly reduced hypoxia-induced neuron death, and significantly increased mitochondrial health in vitro. The results show that 10-HDA has therapeutic effects on brain health during normal development and aging and may combat age and stress-related weight loss [18,19,22]. It has also been found effective against lung injury,

neuroinflammation, immunosuppression, chronic mild stress, hepatotoxicity, osteoarthritis, osteoporosis, melanoma, sarcopenia, Alzheimer disease, cardiovascular diseases, lung cancer and colon Cancer [111].

3. MATERIALS AND METHODS

Table 3.1. The substances, their brand names and codes used during the experiments.

SUBSTANCE	BRAND	CODE
10-HDA (Royal Jelly Acid) (≥98%)	Chem Cruz	sc-281143A
Ketamine (Keta-Control)	Doğa İlaçlar Üretim Paz. İth. İhr. Tic. Şirketi	200932
Xylazine (Rompun)	Bayer	047-956
Vicryl Suture	BSM	348536237
Prolene Suture	BSM	344003995
Castroviejo Needle Holder	Aesculap	BH110R
Povidone Iodine (Batticon)	Adeka	8699587651242
Paraformaldehyde	ICN Biomedicals	150146
PBS tablets	Biomatik	A3602
Poly-L lysine coated slide	PatolLab	165014
Tissue Freezing Medium	Leica	14020108926
Microtome Blades	Leica	14035838925
Sodium Azide	Serva	30175.01
Bovine Serum Albumin	Sigma	A-9418
Triton	Merck	1.08603.1000
Tween 20	Sigma	S8026684 108
BIII Tubulin 488 Conjugated Antibody	Merck Millipore	ab15708a
P0 Rabbit Primer Antibody	Affinity	DF6555
NFH Mouse Primer Antibody	Abcam	ab7795
S100 Rabbit Primer Antibody	Abcam	ab34686
BNG Conjugated Antibody	Invitrogen	B13423
Seconder Antibody Goat Anti Rabbit 568	Thermo Fisher	A11011
Seconder Antibody Goat Anti Mouse 488	Thermo Fisher	A21042
Hydrophobic PAP Pen	PatoLab	PEN-01

3.1. Animals

Ethical approval was obtained for this study with the decision of Van Yüzüncü Yıl University Animal Experiments Local Ethics Committee, dated 25.02.2021 and numbered 2021/02-11. Animal handling and surgical procedures were carried out in ‘‘accordance” with the approved guideline of this commission. Animal material in the study was obtained from Yüzüncü Yıl University Experimental Medicine Application and Research Center. All experiments were performed using male BALB/c mice (6–8 weeks old, 20–25 g) housed in colony cages with free access to food and water and maintained in a standard environment

including a 12 h light/dark cycle, constant room temperature (24 ± 2 °C) and humidity (40–60 %). All surgical and therapeutical processes were performed at Van Yüzüncü Yıl University Experimental Medicine Application and Research Center.

56 animals were included in the study. 40 male mice were assigned for the treatment and functional tests while 16 mice were used separately to verify the success of the crush injury.

3.2. Groups and Treatment

The mice were randomly divided into four groups: sham, crush, 10-HDA 30 mg/kg (HDA 30), and 10-HDA 60 mg/kg (HDA 60). 10-HDA (purity ≥ 98%) was prepared in saline solution [112]. Ultrasonication was applied in order to optimize the solubility of 10-HDA[113]. For the treatment of animals one hour after crush injury, the mice were given 0.9% saline or 10 HDA (30 and 60 mg/kg) orally through flexible gavage daily for four weeks [114].

I. Sham group – no crush injury + saline (n=10)
II. Crush group – crush injury + saline (n=10)
III. HDA 30 group - crush injury + 10-HDA 30 mg/kg/p.o. (n=10)
IV. HDA 60 group - crush injury + 10-HDA 60 mg/kg/p.o. [22] (n=10).

3.3. Surgical Procedure

Surgical procedure and crush injury were performed under general anesthesia (ketamine 100 mg/kg/xylazine 10 mg/kg) and sterile conditions. The lateral area of the left thigh of the mice was shaved, the area was disinfected with 70% alcohol spray, the dissection area was cleaned with povidone iodine, and the sciatic nerve was exposed with a surgical intervention parallel to the leg axis. Except for the sham group, a crush injury was created with an edentulous Castroviejo needle holder 5 mm proximal to the trifurcation point in the sciatic nerves of the animals for 30 seconds (approximately 35 Megapascals of pressure) [115], the sciatic nerves of the animals in the sham group were exposed, however, the nerve was not operated. The muscle incision was sutured with 5/0 vicryl and the skin incision with 5/0 prolene [116]. The validity of the sciatic crush injury model was confirmed by sensory and motor function tests, electromyographic assessment and immunohistochemistry performed.

3.4. Functional Tests

These tests were performed four times during the assay; pre-op (T0) and post-op (T1, T2, T3).

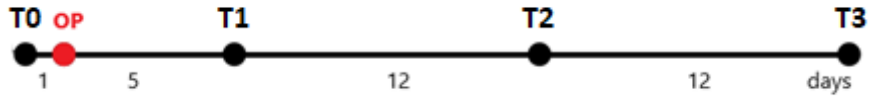

3.4.1. Unilateral Thermal Hyperalgesia Test

The sciatic nerve's sensory function was assessed thanks to the thermal hyperalgesia test. For this test, a painful thermal nociception instrument was used, and the heater plate was set to 55℃. A single mouse's left leg that is planned to be operated, was placed on the hotplate before the operation (T0), and the time from placing the mouse's leg on the hot plate to lifting, shaking, or licking the hind leg was recorded, in seconds, as the reaction time to the painful stimulus. In post-crush (T1), the middle (T2), and at the end (T3) of the study, the lesioned foot of the mouse was contacted unilaterally to the plate. Animals that responded longer than 10 seconds prior to surgery were excluded from the study and replaced with a new animal. To protect the animals' feet from burning, the subjects were not kept on the hot plate for more than 30 seconds. The thermal pain value of these animals was recorded as 30 seconds [117].

3.4.2. Sciatic Function Index

Motor function was assessed using the Sciatic function index (SFI), based on a protocol described by Inserra and collaborators [118]. SFI was calculated by the walking track analysis. Pawprints were registered weekly. The print length (PL), corresponding to the distance from the heel to the third toe, and the toe spread (TS), corresponding to the distance from the first to the fifth toe. Measurements were taken from injured (E, from experimental) as well as uninjured (N, from normal) sides. The mouse's right hind leg (Intact-Normal [N]) and left hind leg (experimental [E]) were dipped in a wet sponge with black ink, the mice were placed in a dark boxed 50 cm X 4 cm walkway, allowed to walk on the white paper covered walkway. PL and TS were measured from the footprint of both the normal side and the experimental side. SFI was calculated according to the following equation: SFI = 118.9 x [(ETS – NTS)/NTS] – 51.2 x [(EPL – NPL)/ NPL] – 7.5 [117].

3.4.3. Horizontal Ladder Rung Walking Test

The ladder rung task was previously applied on rats [119] and thereafter was successfully adapted and applied to mice [120]. This test is both a sensory and motor function test. The horizontal ladder rung walking test (HLRWT) has been used to evaluate walking ability in mice, and measure both forelimb and hindlimb placing, stepping, and inter-limb co-ordination [119]. We aimed to characterize gait impairment of the sciatic crush damage and gait recovery of 10HDA-treated sciatic nerve using HLRWT. The device consists of two plexiglass walls (70 cm x 16 cm). The walls were spaced 40 mm apart to allow for passage of a mouse but prevent it from turning around. The metal steps are 2 mm in diameter and 40 mm in length. The ladder was elevated 11 cm above the ground. The distance between the steps was changed, and an irregular step pattern was created. Foot placement, stepping, and walking performances of the animals were recorded with a video camera system that shoots from a slightly ventral angle placed and fixed on the side of the ladder. A qualitative assessment of experimental hindlimb placement was made using the scoring system.

Ladder task analysis: The following scale was used adapted from Metz [119].

(0) Total miss. Limb doesn't touch a rung and causes a fall. Fall disturbs body weight support, stepping cycle is interrupted.

(1) Deep slip. Limb is placed on a rung, then slips off while weight-bearing, causes animal to fall.

(2) Slight slip. Limb is placed on a rung and then slips; however, no fall is observed. Animal continues walking.

(3) Replacement. Limb contacts on a rung, however, is subsequently moved and replaced on another rung.

(4) Correction. The limb aims for one rung, doesn't touch on it, then replaced on another rung.

(5) Partial placement. The limb is placed on a rung with heel or toes. The limb is fully weight-bearing.

(6) Correct placement. The stepping limb is placed on a rung with all of the palm, digits wrapped around the rung. The limb is fully weight bearing

All video recordings were analyzed frame-by-frame. Each step during a pass down the ladder was scored, however, the first two initiation steps and last two final steps were omitted when an animal paused. Each step was scored according to the quality of limb placement. The average step score was calculated by dividing the total points obtained by the animals from each step after 1 round by the number of steps taken for each animal in 1 round, and statistically

compared between the groups. The day before the test, the animals were allowed to walk for two minutes on the steps of the stairs to familiarize themselves with the test apparatus. Tests were carried out before the operation (T0) and during treatment (T1, T2 and T3) [119].

3.4.4. Rotarod

For motor coordination analysis, we used the rotarod test device (Ugo Basile, Comerio VA, Italy). One day before the test, the mice were accustomed to the test at 5 rpm. The next day, the device was worked with a module that would reach acceleration from 4 rpm to 40 rpm in 5 minutes. Tests were carried out before the operation (T0) and during treatment (T1, T2, and T3). The time until the first falls of the animals was taken into account. Animals were not kept on the mile for more than 300 seconds[121].

3.5. EMG

This test was performed under general anesthesia, at 37°C body temperature, and in an environment isolated from environmental electromagnetic waves (in a Faraday cage) with an EMG device (Nihon Kohden, Japan). Motor nerve conduction examination is a key method for assessing motor axon regeneration and muscle innervation. Motor nerve conduction velocity (MNCV) is used to reliably determine the speed at which the impulse generated in large, myelinated nerve fibers transmit the signal via axons to the distal nerves and muscles.

In this study, stimulations and recordings were performed in the experimental standing. Proximal stimulus (PS) was applied on level of supramaximal to the sciatic notch, 5 mm proximal to the injury site with two silver electrodes, and response was received from the lateral plantar muscles. The distal stimulus was given from the elbow (ankle), and the response was again received from the lateral plantar muscles. Compound muscle action potential (CMAP) values were measured from the center of the gastrocnemius muscle. Proximal and distal latency values were measured from the lateral plantar muscles. The distance (millimeters) between the stimulus points (sciatic notch and ankle) was divided by the latency difference (proximal and distal) and motor nerve conduction velocity (MNCV) (meters/second) was calculated. Damage/repair/functional recovery level was evaluated [117]. The gold standard tests for evaluating peripheral nerve repair and functional recovery in the extremities are electromyography and nerve conduction studies [6].

3.6. Immunohistochemistry

In order to understand the microstructural changes of the crushed sciatic nerve; immunohistochemical staining, imaging, and analysis were carried out.

3.6.1. Tissue Section's Preparation

Sciatic nerves and Gastrocnemius muscles were freshly dissected, embedded, and frozen at -20^{o}C. Sections fixed in cold 4% paraformaldehyde. Then, they were kept in 30% sucrose solution prepared in phosphate buffer solution (PBS) for 24 hours. With the Cryostat-Frozen device, 10 µm longitudinal sections from sciatic nerve tissue and 18 µm longitudinal sections from soleus muscle were taken on poly-L lysine-coated slides. The slides were treated with block solution (0.1% Triton-X, 3% bovine serum albumin, 0.1% sodium azide in PBS) for 30 minutes [122].

3.6.2. Immunofluorescence Staining

Primary antibodies used: Anti-tubulin beta III antibody (1/100, 488 conjugated, Millipore-ab15708a), monoclonal mouse anti-neurofilament heavy polypeptide antibody (1/100, 488, Abcam-ab7795), polyclonal rabbit anti-myelin protein P0 antibody (1/25, 568, Affinity- DF6555), α- bungarotoxin (1/25, 594 conjugated, Invitrogen-b13423), polyclonal rabbit anti-s100 antibody (1/100, 568, Abcam-ab34686).

Secondary antibodies used: Alexa fluor 568 - 1/100 goat anti-rabbit IgG (1/100, Thermo Fisher A-11011), Alexa fluor 488 - goat anti-mouse IgG (1/100, Thermo Fisher A-21042**)**.

The nerve section's slides were incubated with primary antibodies (anti-neurofilament-200 antibody, anti-βIII-tubulin antibody, anti-S100 antibody, anti-myelin protein P0 antibody, α- bungarotoxin) in 0,1% Tween 20, 0,1% sodium azide and 3% bovine serum albumin for 1 h at +4 ℃ for 1 night in a humid environment [122]. After washing, the slides were incubated with secondary antibodies (goat anti-rabbit 568, goat anti-mouse 488) in 0,1% Tween 20, 0,1% sodium azide and 3% bovine serum albumin for one h at +4 ℃ [123]. The muscle section's slides were incubated with Alexa Fluor 594 conjugated bungarotoxin.

To view the changes in axon integrity, neurofilament (NFH) antibody [124] and βIII-

tubulin antibody (βIII) [125]; to view changes in myelin structure, myelin protein zero (P0) antibody [126]; to detect changes in acetylcholine receptor of the motor endplate at the neuromuscular junction, α-bungarotoxin antibody (BNG) [44]; and to assess the numerical intensity and activation of Schwann cells, the S100 antibody [122] was used.

3.7. Laser Scanning Confocal Microscopic Imaging and Analysis

After washing three times with PBS, immunohistochemically stained preparations were visualized under a laser scanning confocal microscope (LSM 510 META-Zeiss). Images were captured using an Axioscobe camera and recorded in the appropriate multitrack processing mode to show multiple fluorescent radiations simultaneously.

3.7.1. Wavelengths and Lasers

Argon (488 nm) and helium-neon (543 nm) lasers were used for imaging.

3.7.2. Software

Fluorescent images taken with a laser scanning confocal microscope and LSM 3.0 [117] software were analyzed and compared with the ImageJ program. ImageJ is a pixel quantity-based program which is been used widespread in the immunohistochemistry field [127]. The Axiovision software was used to process images.

3.8. Statistical Analysis

R Studio program was used for statistical calculations and analysis. Descriptive statistics for the following features; Expressed as Median, Standard Deviation, Minimum and Maximum values. The distribution of the samples and the homogeneity of the variances were controlled. The presence of the outliers has shown that non-parametric tests should have been applied for these statistical analyses. The Kruskal-Wallis analysis was used to compare groups. Afterwards Mann-Whitney U test was applied to compare the difference between two groups for each week (Sham-Crush, Crush-HDA 30, Crush-HDA 60 and HDA30-HDA60 groups). The time dependent repeated measure comparison for one group was calculated with Friedman test. Afterwards, Wilcoxon test was applied to compare the difference between 2 weeks for each group (T0-T1, T1-T2, T2-T3, T0-T3). The results obtained in the study were summarized using

the median±standard deviation as descriptive statistics, and the statistical significance level is indicated according to their p values: p<0,001=*** or ###, p<0,01=** or ## and p<0,05=* or #.

4. RESULTS

4.1. The Effect Of 10-HDA on Thermal Hyperalgesia in Hot-Plate Test in Mice

The thermal hyperalgesia test was performed four times, 1 pre-op and 3 post-op. T0: 1st day, T1: 6th day, T2: 18th day and T3: 30th day. The results of the four assays are shown in Table 4.1., Figure 4.1. and Figure 4.2.

Table 4.1. The statistical comparison of thermal hyperalgesia median latency values (seconds) and standard deviations per group for each week.

	T0		T1		T2		T3	
	Median	St. Dev.	Median	St. Dev.	Median	St. Dev.	Median	St. Dev.
SHAM	6,32	0,75	7,58	2,53	6,83	3,34	5,40	2,69
CRUSH	7,25	1,73	29,58	0,89	24,88	5,94	13,31	8,38
HDA 30	6,53	1,22	25,91	5,07	14,31	4,93	8,90	3,06
HDA 60	5,55	1,83	25,50	6,96	15,86	5,50	10,40	3,59

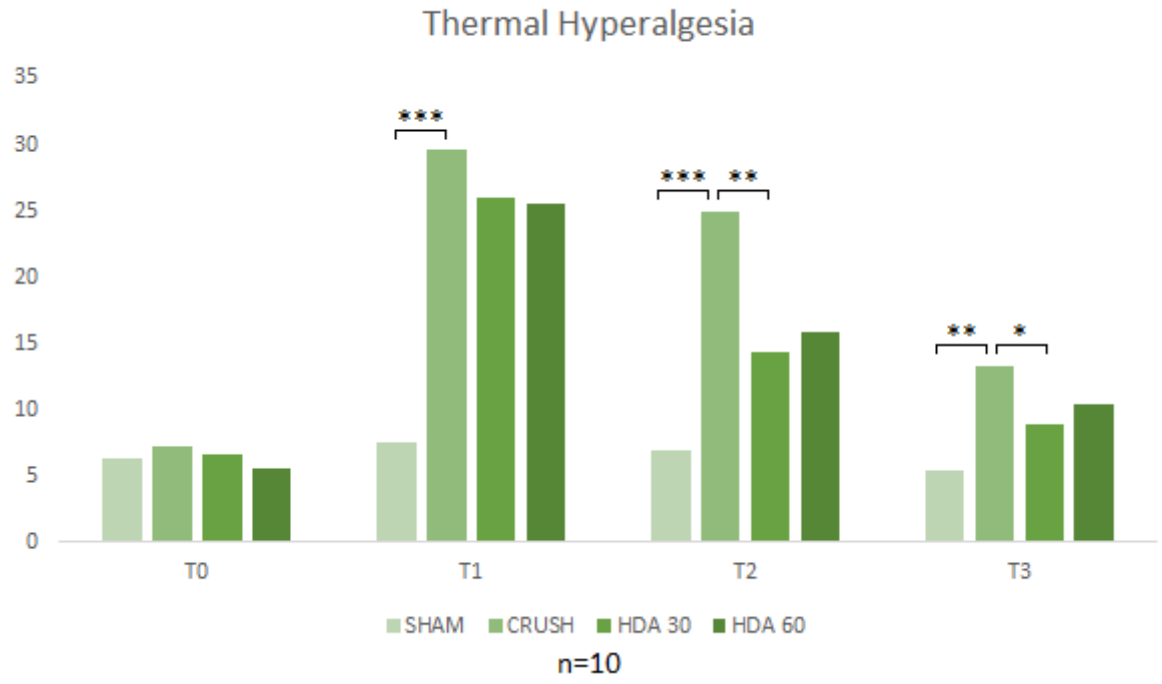

Figure 4.1. Graphical view of the comparison of thermal hyperalgesia latency medians values between groups for each week. The statistical significance level is indicated according to their p values: p<0,001=*** or ###, p<0,01=** or ## and p<0,05=* or #.

Before crush injury (T0), the findings did not show statistically significant difference between the groups. The results after crush injury (T1) indicated that the latencies of sham and

crush groups had a statistically significant difference (p<0,001) (Table 4.1., Figure 4.1).

The T2 findings revealed that the latency of sham and crush groups were statistically significantly different from each other (p<0,001). Sham and HDA 30 groups had a statistically significant difference (p< 0,01). HDA 30 and HDA 60 groups had no statistically significantly difference between each other (Table 4.1., Figure 4.1).

The T3 findings showed that the crush group had the longest latency. The latency of the crush group was significantly longer than the sham group (p<0.01). The latency of crush and HDA 30 group had a statistically significant difference (p<0,05). There was no statistically significant difference between HDA 30 and HDA 60 groups (Table 4.1., Figure 4.1).

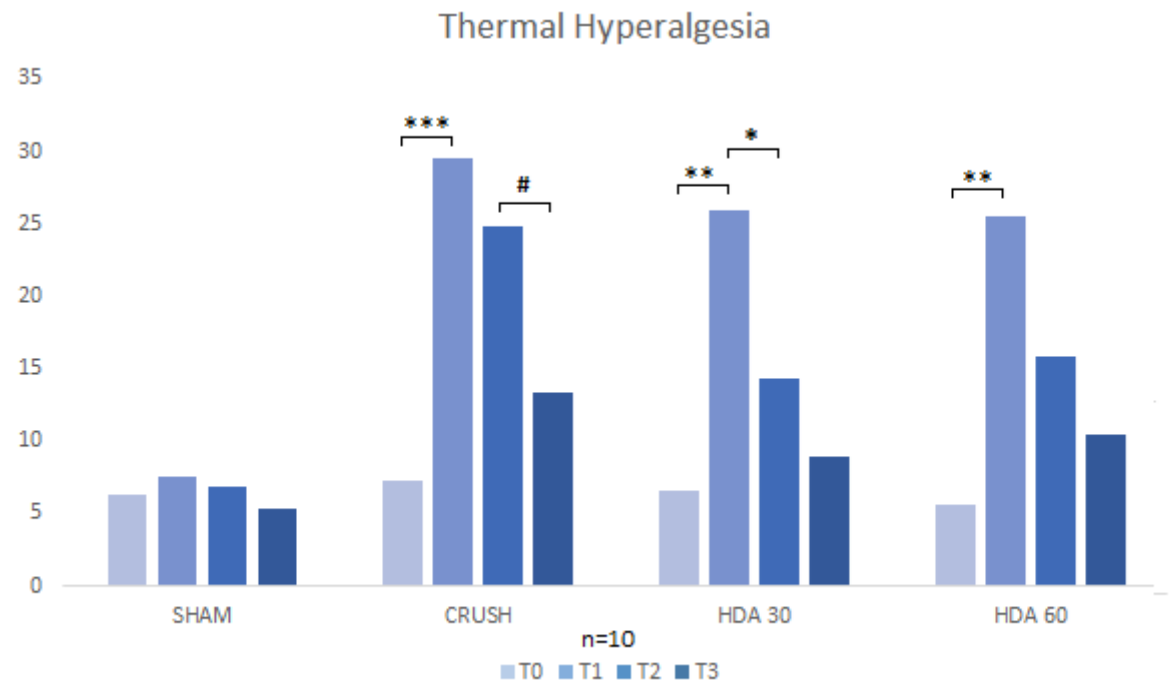

Figure 4.2. Graphical view of the comparison of thermal hyperalgesia latency medians values between weeks for each group. The statistical significance level is indicated according to their p values: p<0,001=*** or ###, p<0,01=** or ## and p<0,05=* or #.

Sham group had no statistically significant difference between tests during the experiment. For the crush group, there was a statistically significant difference between T0 and T1 (p<0,001). T1 and T2 tests had no statistically significant difference. The thermal hyperalgesia latency of T2 and T3 tests had a statistically significant difference (p<0,05). There was no statistically significant difference between T0 and T3 tests. HDA 30 group had a statistically significant difference between T0 and T1 tests (p<0,01). There was also a

statistically significant difference between T1 and T2 tests ($p<0,05$). T2 and T3 tests had no statistically significant difference. There was also no statistically significant difference between T0 and T3 tests. HDA 60 groups latency showed a statistically significant difference between T0 and T1 tests $p<0,01$). There was no statistically significant difference between T1-T2 or T2-T3 or T0-T3 trials (Figure 4.2.).

4.2. The Effect of 10-HDA on Sciatic Functional Index

The results of the sciatic functional index were calculated with walking track analysis performed in T0, T1, T2, and T3. T0: 1st day, T1: 6th day, T2: 18th day and T3: 30th day. Median values for the SFI are shown in Table 4.1., Figure 4.1.

Table 4.2. The statistical comparison of sciatic function index median values for each week.

	T0		T1		T2		T3	
	Median	St.Dev	Median	St.Dev	Median	St.Dev	Median	St.Dev
SHAM	-9,49	3,41	-26,05	9,08	-27,01	10,61	-15,12	7,22
CRUSH	-11,92	2,96	-73,24	11,92	-60,21	14,73	-35,55	11,15
HDA 30	-11,64	2,98	-55,65	20,52	-36,87	21,41	-15,58	12,35
HDA 60	-11,77	3,15	-47,08	23,62	-41,37	20,98	-24,01	19,69

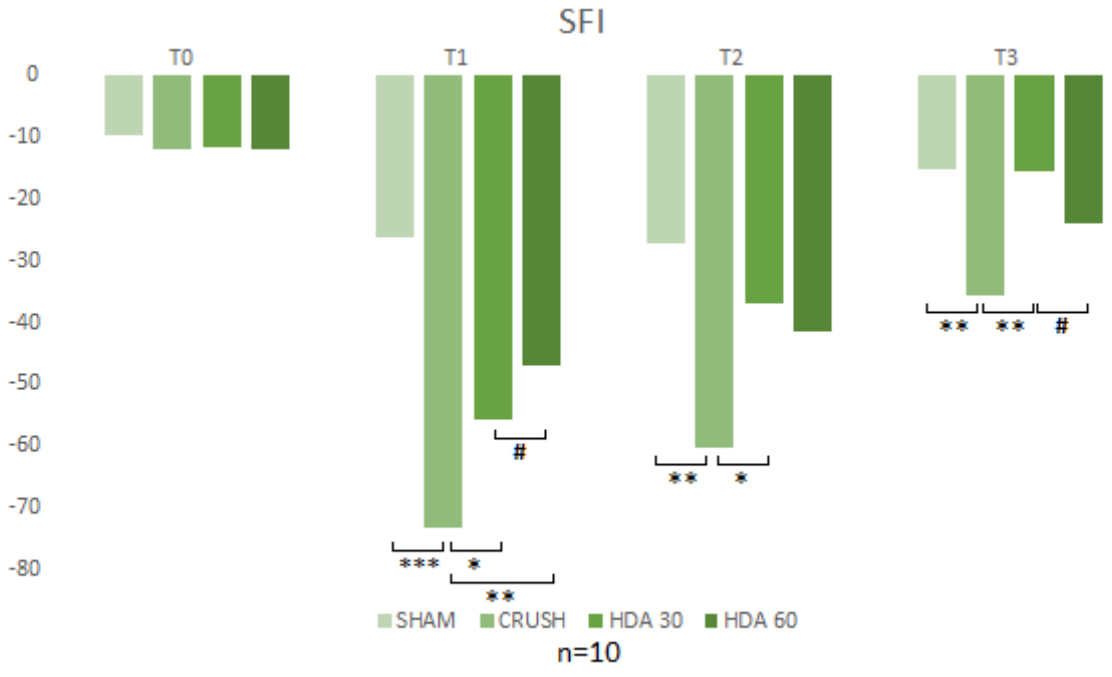

Figure 4.3. Graphical view of the comparison of sciatic function index median values between groups for each week. The statistical significance level is indicated according to their p values:

p<0,001=*** or ###, p<0,01=** or ## and p<0,05=* or #.

There was no significant difference between the groups at T0 (Table 4.2., Figure 4.3).

The results at T1 indicated that the SFI values of the sham and crush group had a statistically significant difference (p<0,001), and the SFI value of the crush group was significantly worse in comparison with HDA 30 group (p<0.05), HDA 60 group had significantly better performance than the crush group (p<0.01). HDA 60 group had a scientifically significant higher SFI in comparison with HDA 30 group (p<0,05) (Table 4.2., Figure 4.3).

The results at T2 revealed that the sham group has a significantly better SFI value than the crush group (p<0.01). There was no statistically significant difference among the Crush, HDA 30, and HDA 60 groups. HDA 30 group had a scientifically significant higher SFI than crush group (p<0,05), however, there was no statistically significant difference between the HDA 30 and HDA 60 groups (Table 4.2., Figure 4.3).

The findings at T3 revealed that the SFI performance of the sham group and the HDA 30 group were significantly better than the crush group (p<0.01). HDA 30 group had a statistically significant higher SFI than HDA 60 group (p<0,05). The HDA 60 group had a statistically significant higher SFI level than crush group (p<0,05) (Table 4.2., Figure 4.3).

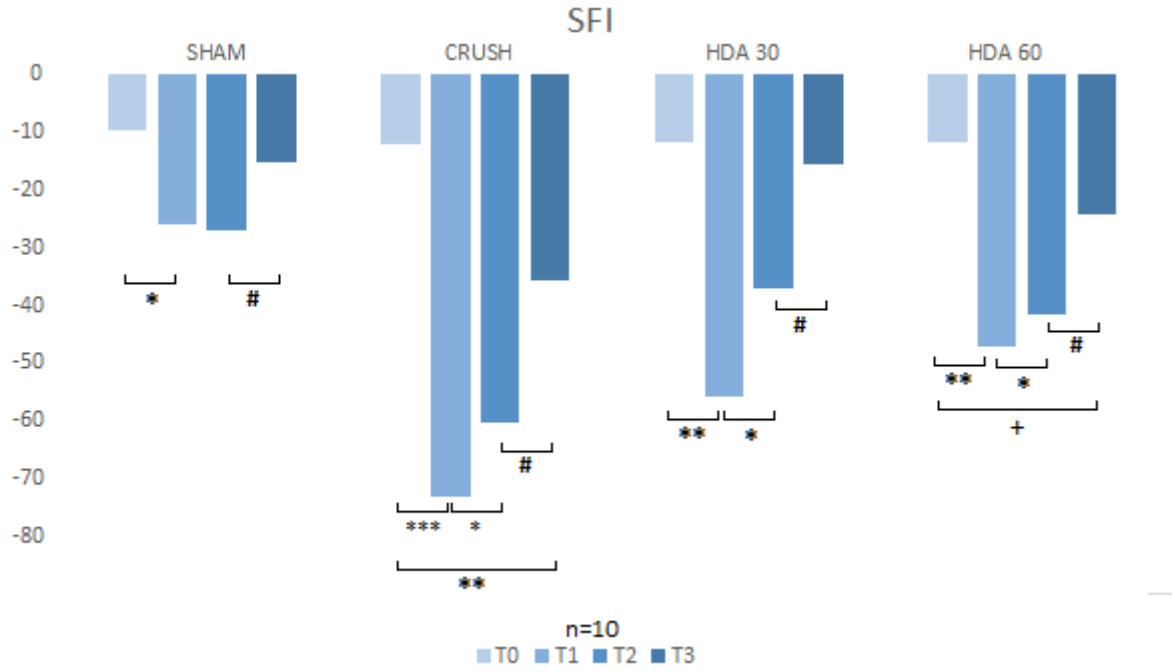

Figure 4.4. Graphical view of the comparison of sciatic function index median values between weeks for each group. The statistical significance level is indicated according to their p values:

p<0,001=*** or ###, p<0,01=** or ## and p<0,05=*, # or +.

Sham group had a statistically significant difference between T0 and T1 tests (p<0,05). Also, T3 tests showed scientifically significant better SFI level than T2 (p<0,05). The crush groups T0 data had a scientifically significant higher SFI level in comparison with T1 (p<0,001). T2 data showed a scientifically significant higher SFI level in comparison with T1 (p<0,05) and T3 data showed a scientifically significant higher SFI level in comparison with T2 (p<0,05). T0 data had a scientifically significant higher SFI level in comparison with T3 (p<0,01) (Figure 4.4.).

HDA 30 group's T0 data showed scientifically significant better SFI level than T1 (p<0,01), T2 data showed scientifically significant better SFI level than T1 (p<0,05) and T3 showed scientifically significant better SFI level than T2 (p<0,05). There was no scientifically significant difference between T0 and T3 tests (Figure 4.4.).

HDA 60 group's T0 data showed scientifically significant better SFI level than T1 (p<0,01), T2 data showed scientifically significant better SFI level than T1 (p<0,05) and T3 showed scientifically significant better SFI level than T2 (p<0,05). T0 data showed scientifically significant better SFI level than T3 (p<0,05) (Figure 4.4.).

4.3. The Effect of 10-HDA on Horizontal Ladder Rung Walking Test

The horizontal ladder rung walking test (HLRWT) was performed in T0, T1, T2, and T3. T0: 1st day, T1: 6th day, T2: 18th day and T3: 30th day. Median scores for the HLRWT are shown in Table 4.3. and Figure 4.3.

Table 4.3. The statistical comparison of HLRWT median values for each week.

	T0		T1		T2		T3	
	Median	St.Dev	Median	St.Dev	Median	St.Dev	Median	St.Dev
SHAM	5,80	0,16	5,77	0,31	5,92	0,18	5,66	0,35
CRUSH	5,79	0,22	2,85	1,10	5,46	0,66	5,69	0,23
HDA 30	5,76	0,33	3,24	0,89	5,66	0,53	6	0,24
HDA 60	5,93	0,31	2,82	1,17	5,67	0,39	6	0,33

Figure 4.5. Graphical view of the comparison of HLRWT median values between groups for each week. The statistical significance level is indicated according to their p values: p<0,001=*** or ###, p<0,01=** or ## and p<0,05=* or #.

The results at T0 indicated no statistically significant difference between the groups (Table 4.3., Figure 4.5).

The results at T1 indicated that the crush group had significantly weaker walking functions than the sham group (p<0.01). There was no statistically significant difference between the crush, HDA 30, and HDA 60 groups (Table 4.3., Figure 4.5).

The results at T2 showed a significantly worse walking performance in the crush group compared to the sham group (p<0,01). The HDA 30 group had a statistically significant higher walking function than crush group (p<0,05). There was no statistically significant difference between the HDA 30 and the HDA 60 groups (Table 4.3., Figure 4.5).

The results at T3 indicated no statistically significant difference between the groups (Table 4.3., Figure 4.5).

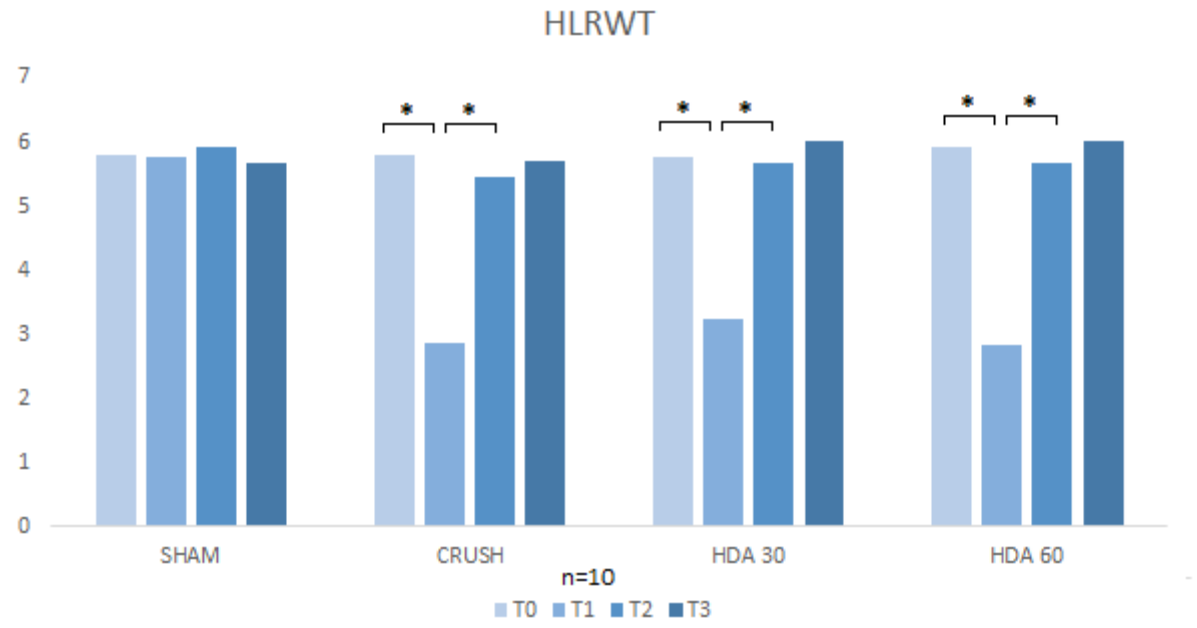

Figure 4.6. Graphical view of the comparison of HLRWT median values between weeks for each group. The statistical significance level is indicated according to their p values: p<0,001=*** or ###, p<0,01=** or ## and p<0,05=* or #.

Sham group didn't have statistically significant difference between any tests. Crush group's T0 test showed scientifically significant higher HLRWT level than T1 (p<0,05). T2 and T3 tests showed scientifically significant higher HLRWT level than T1 (p<0,05). HDA 30 group's T0 test showed scientifically significant higher HLRWT level than T1 (p<0,05). T2 and T3 tests showed scientifically significant higher HLRWT level than T1 (p<0,05). HDA 60 group's T0 test showed scientifically significant higher HLRWT level than T1 (p<0,05). T2 and T3 tests showed scientifically significant higher HLRWT level than T1 (p<0,05) (Table 4.3., Figure 4.6).

4.4. The Effect of 10-HDA on Rotarod Staying Time in Sciatic Nerve Crush Injury Model

Rotarod testing was carried out at T0, T1, T2, and T3. T0: 1st day, T1: 6th day, T2: 18th day and T3: 30th day. Motor performance was considered the latency to fall off the rotarod apparatus determined from the meantime in three trials for each mouse. For each test, the latencies of falling off the rotarod were recorded. The latencies to fall off the rotarod are shown in Table 4.4 and Figure 4.4.

Table 4.4. The statistical comparison of rotarod staying time median values (seconds) for each week.

	T0		T1		T2		T3	
	Median	St.Dev	Median	St.Dev	Median	St.Dev	Median	St.Dev
SHAM	71,67	15,20	75,33	20,83	66,33	20,74	57,67	22,95
CRUSH	76,33	14,47	41,67	25,35	31,33	9,30	36	5,47
HDA 30	76	10,32	45,50	21,05	47,17	17,20	56,67	29,46
HDA 60	80	10,01	47,67	23,54	53,67	25,76	63	24,67

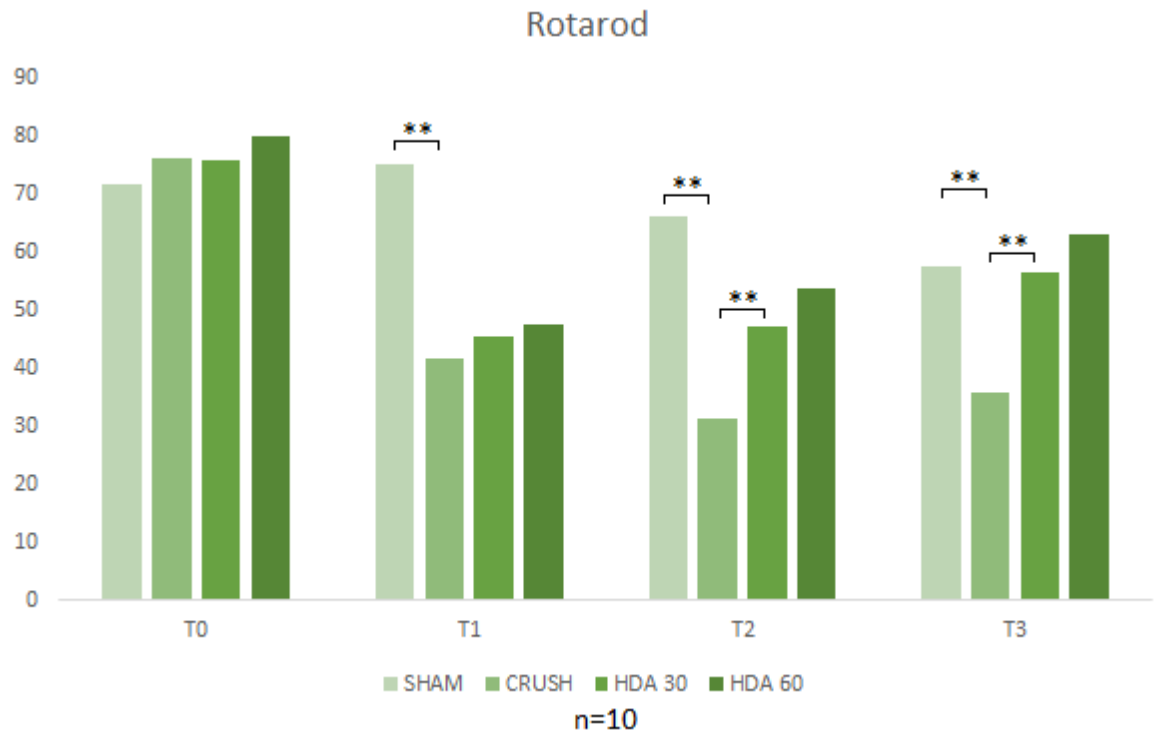

Figure 4.7. The graphical view compares median rotarod values (seconds) between groups for each week. The statistical significance level is indicated according to their p values: p<0,001=*** or ###, p<0,01=** or ## and p<0,05=* or #.

At T0, Rotarod findings indicated no statistically significant difference between the groups (Table 4.4., Figure 4.7).

The findings at T1 stated that the motor performance of the sham group had a scientifically significant higher level than crush group (p<0,01). Crush, HDA 30, and HDA 60

groups had no statistically significant between each other (Table 4.4., Figure 4.7).

The findings at T2 revealed that the motor function of the sham group was scientifically significantly higher than the crush group (p<0.01). HDA 30 group had a scientifically significantly higher level than crush group (p<0,01). There was no statistically significant difference between HDA 30, and HDA 60 groups (Table 4.4., Figure 4.7).

The results at T3 had similar results to T2. The findings at T2 revealed that the motor function of the sham group was scientifically significantly higher than the crush group (p<0.01). HDA 30 group had a scientifically significantly higher level than crush group (p<0,01). There was no statistically significant difference between HDA 30, and HDA 60 groups (Table 4.4., Figure 4.7).

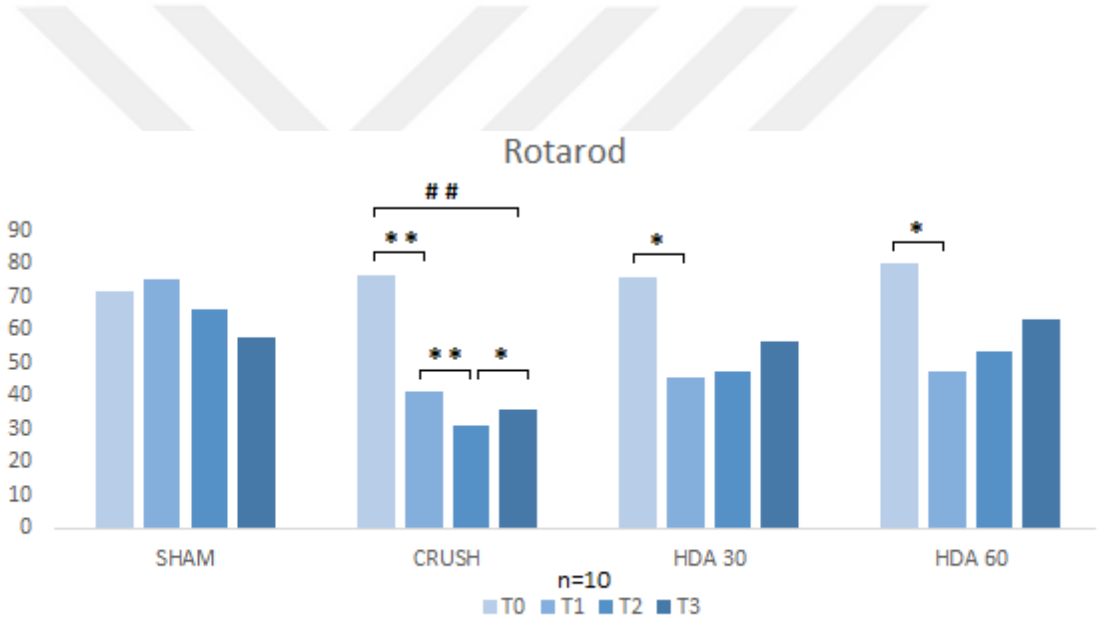

Figure 4.8. The graphical view compares median rotarod values (seconds) between weeks for each group. The statistical significance level is indicated according to their p values: p<0,001=*** or ###, p<0,01=** or ## and p<0,05=* or #.

Sham group didn't have statistically significant difference between any tests. Crush group's T0 test showed scientifically significant higher rotarod latency level than T1 (p<0,01). T1 showed scientifically significant higher rotarod latency level than T2 (p<0,01). T3 showed scientifically significant higher rotarod latency level than T2 (p<0,05). T0 showed scientifically significant higher rotarod latency level than T3 (p<0,01) (Table 4.4., Figure 4.8).

HDA 30 group's T0 test showed scientifically significant higher rotarod latency level than T1 (p<0,05). T1, T2 and T3 groups didn't have any scientifically significant difference

between each other (Table 4.4., Figure 4.8).

HDA 60 group's T0 test showed scientifically significant higher rotarod latency level than T1 ($p<0,05$). T1, T2 and T3 groups didn't have any scientifically significant difference between each other (Table 4.4., Figure 4.8).

4.5. The Effect of 10-HDA on Functional Recovery of Crushed Sciatic Nerve Using Electromyography Tests

EMG tests were performed at the end of the study. Onset Latency, Compound Muscle Action Potential (CMAP), and Motor Nerve Conduction Velocity (MNCV) parameters were evaluated. Electromyographic findings have been shown in Table 4.5 and Figure 4.9.

Table 4.5. The statistical comparison of median EMG values (Latency, CMAP, and MNCV) and standard deviations per group.

	Latency (ms)		**CMAP (mV)**		**MNCV (m/s)**	
	Median	Std. Dev.	Median	Std. Dev.	Median	Std. Dev.
SHAM	1,88	0,30	47,77	14,73	35,37	8,81
CRUSH	3,54	0,62	36,94	9,28	17,26	3,54
HDA 30	2,96	0,71	43,53	14,30	22,65	7,48
HDA 60	2,93	0,48	38,74	7,67	25,17	9,25

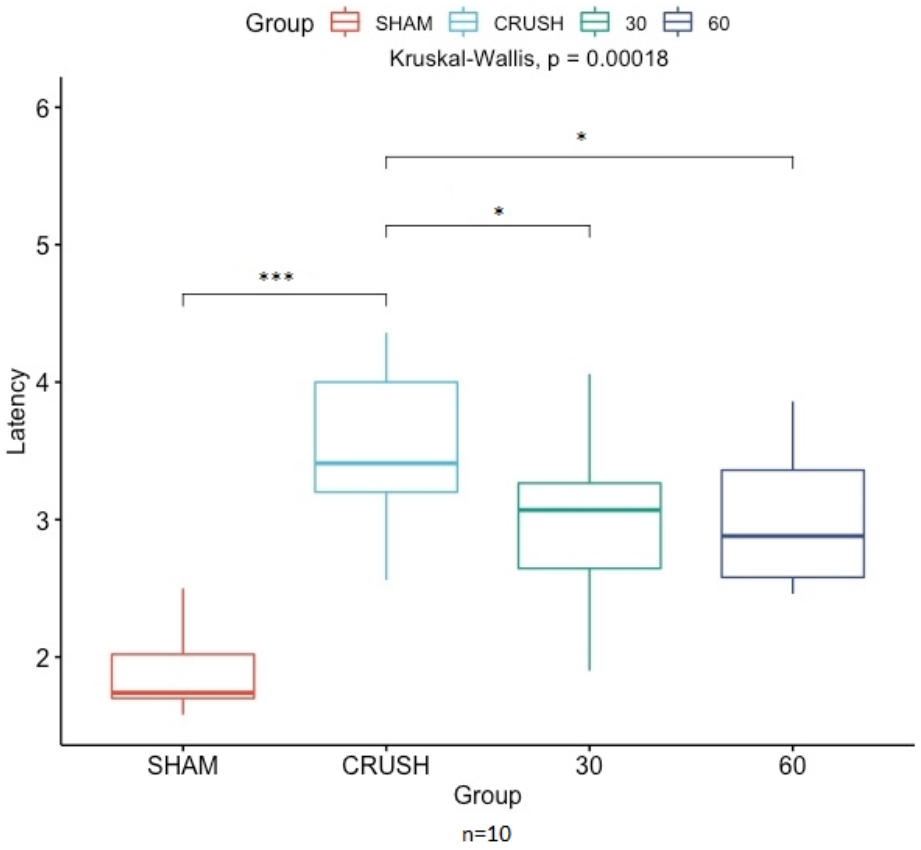

Figure 4.9. Graphical view of the comparison of average latency (millisecond) between groups. The statistical significance level is indicated according to their p values: p<0,001=*** or ###, p<0,01=** or ## and p<0,05=* or #.

The latency measurement results revealed that sham group had a scientifically significant faster latency than crush group (p<0,001). Crush group had a scientifically significant slower latency than HDA 30 group (p<0,05). Crush group had a scientifically significant slower latency than HDA 60 group (p<0,05). HDA 30 and HDA 60 groups had no scientifically significant between each other (Table 4.5., Figure 4.9).

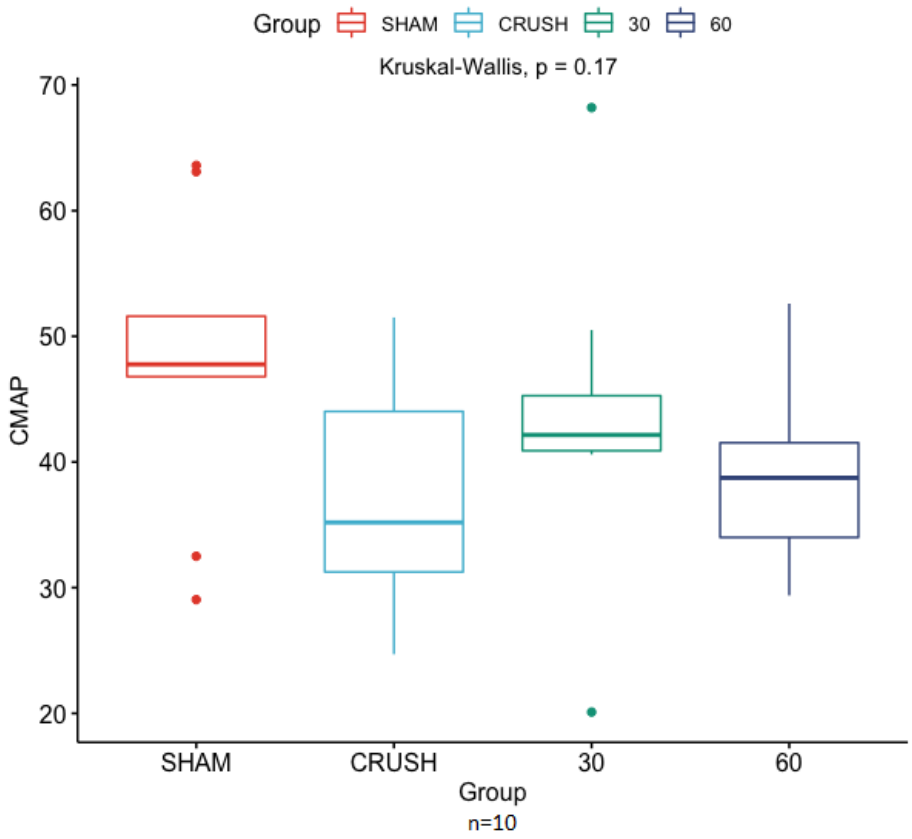

Figure 4.10. The graphical view compares CMAP amplitude values (millivolts) between groups. The statistical significance level is indicated according to their p values: p<0,001=*** or ###, p<0,01=** or ## and p<0,05=* or #.

The CMAP amplitude reflects the number of functional axons. In this study, we evaluated the effect of 10 HDA on the CMAP performance in the sciatic nerve injury model. The peak-to-peak amplitude for the CMAP response was determined.

The CMAP results indicated no statistically significant difference between the Sham, Crush, HDA 30, and HDA 60 groups (Table 4.5., Figure 4.10.).

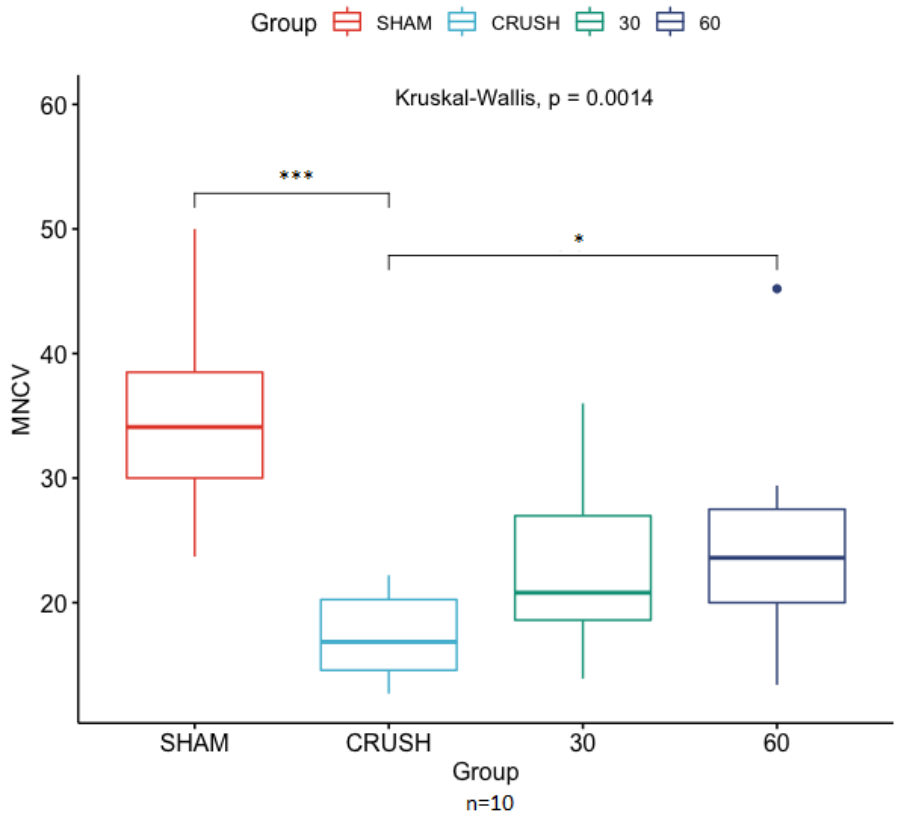

Figure 4.11. The graphical view compares MNCV values (meter/seconds) between groups. The statistical significance level is indicated according to their p values: p<0,001=*** or ###, p<0,01=** or ## and p<0,05=* or #.

The MNCV is determined by the degree of myelination. MNCV was calculated by dividing the distance between the stimulating and recording electrode by subtracting the distal latency from the proximal latency.

The MNCV results showed that the nerve conduction speed of the sham group was scientifically significantly higher than the crush group (p<0.001). The HDA 60 group was scientifically significantly higher than the crush group (p<0,05). HDA 30 and HDA 60 groups didn't have a scientifically significant difference between each other (Table 4.5., Figure 4.11).

4.6. Morphological Evaluation of Regenerative Effect of 10-HDA on Crushed Sciatic Nerve Using Immunohistochemistry and Immunofluorescence

Immunocytochemical method-stained sciatic nerve and gastrocnemius muscle sections were examined using a confocal laser scanning microscope. Pixel intensities of the images were quantified with the Image J program. It was assessed five proteins total to study axonal and

neuromuscular junction constituents. These proteins consist of Neurofilament Heavy Chain 200 (NFH), Beta-III Tubulin (B-III), Schwann protein S100, Myelin Protein 0 (P0), and the Acetylcholine receptor (stained with α-Bungarotoxin - BNG). The NFH, B-III, S100, and P0 proteins were stained on the sciatic nerve. The BNG and NFH were stained on the Gastrocnemius muscle. The NFH staining was named NFH-M (Muscle) and NFH-N (Nerve).

The median pixel values of all the immunostaining images (P0, BIII, BNG, NFH-M, NFH-N, and S100) are shown in Table 4.6, and Figure 4.12-4.17. The microscopy images of all immunostainings are shown in Figure 4.18-20.

Table 4.6. The statistical comparison of median pixel values and standard deviations per group.

	P0		BIII		BNG		NFH-M		NFH-N		S100	
	Median	St. Dev.	Median	St. Dev.	Median	St. Dev.	Median	St. Dev.	Median	St. Dev.	Median	St. Dev.
SHAM	23,74	3,19	54,83	3,12	14,87	0,57	14,35	1,11	59,99	1,37	63,11	6,49
CRUSH	9,73	1,3	27,9	0,62	9,55	1,53	6,86	1,2	36,77	7,96	13,84	1,76
HDA 30	23,63	2,04	39,6	3,32	12,7	2,43	14,56	2,13	61,21	14,63	31,19	4,44
HDA 60	25,06	1,46	29,32	3,49	14,31	0,58	11,94	1,15	40,6	1,24	75,96	1,58

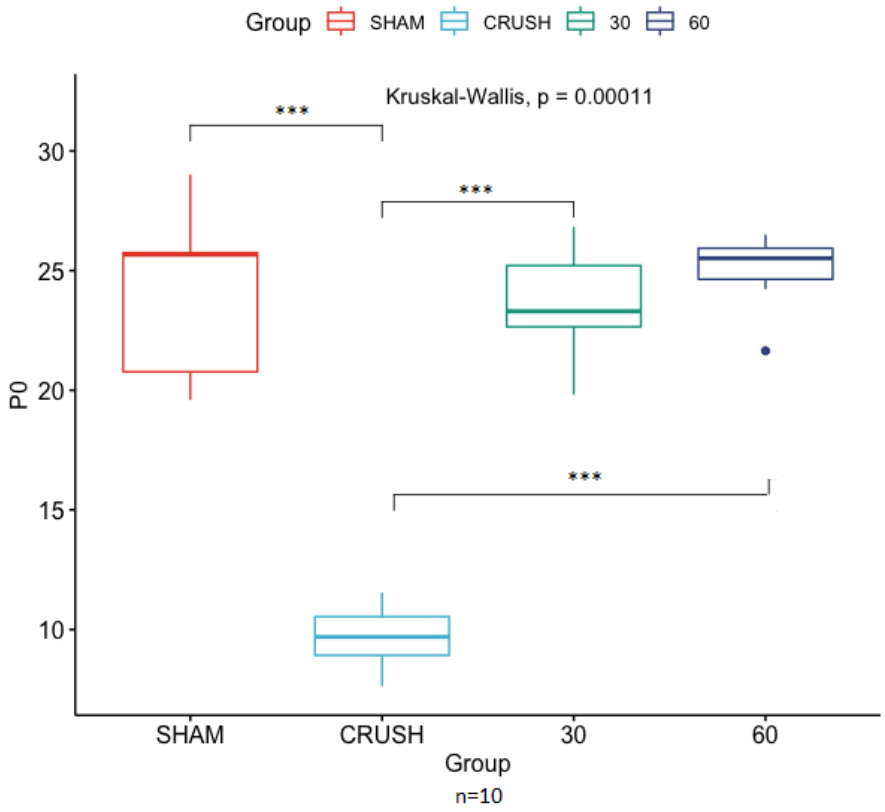

Figure 4.12. Graphical view of the comparison of the median pixel intensity of P0 between groups. The statistical significance level is indicated according to their p values: p<0,001=*** or ###, p<0,01=** or ## and p<0,05=* or #.

Myelin protein zero (P0) is an integral membrane glycoprotein and a major peripheral nervous system myelin structural component.

P0's pixel intensity of sham group was significantly higher than the crush group (p=0,001). HDA 30 group had a statistically significant higher P0 pixel intensity in comparison with crush group (p<0,001). HDA 60 group had a statistically significant higher P0 pixel intensity in comparison with crush group (p<0,001). HDA 30 and HDA 60 groups didn't have a statistically significant difference between each other (Table 4.6, Figure 4.12, and Figure 4.18).

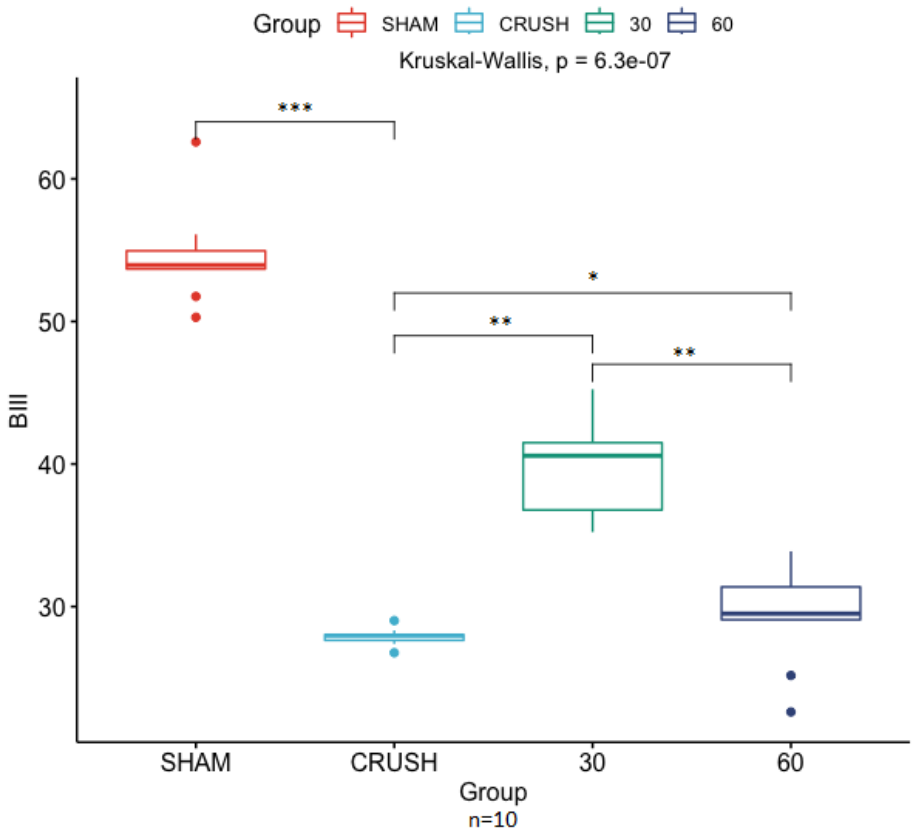

Figure 4.13. The graphical view compares the median pixel intensity of the BIII between groups. The statistical significance level is indicated according to their p values: p<0,001=*** or ###, p<0,01=** or ## and p<0,05=* or #.

The pixel intensity of the BIII tubulin, an axon marker in the sciatic nerve, was significantly higher in the sham group in comparison with the crush group (p=0.001). The pixel intensity of the BIII tubulin in the HDA 30 group was scientifically significantly higher than crush group (p=0.01). The pixel intensity of the BIII tubulin in the HDA 60 group was scientifically significantly higher than crush group (p<0,05). The pixel intensity of the BIII tubulin in the HDA 30 group was scientifically significantly higher than HDA 60 group (p<0,01) (Table 4.6, Figure 4.13, and Figure 4.18).

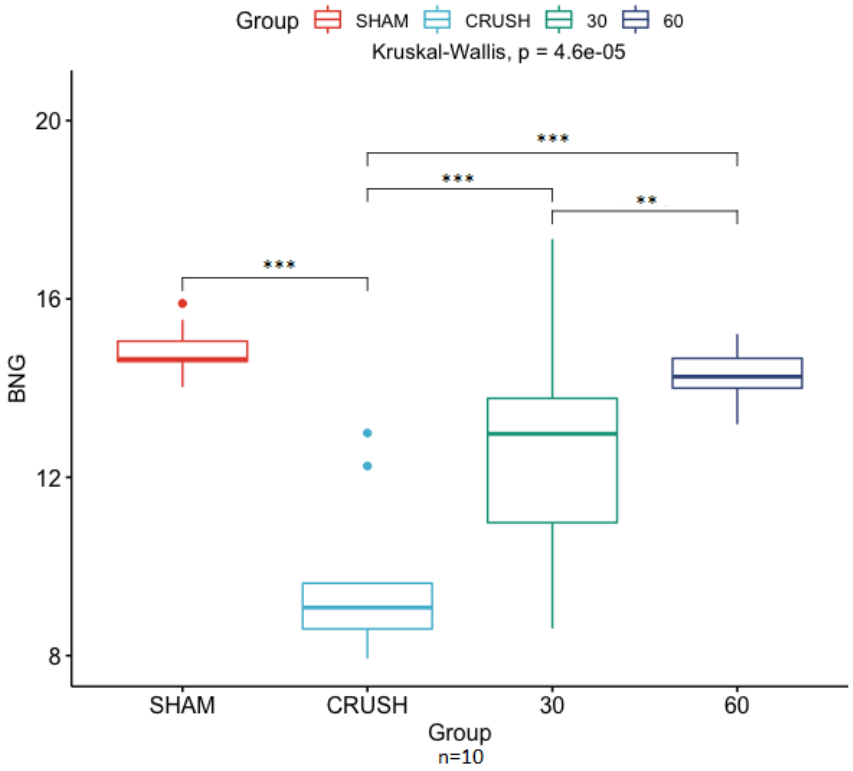

Figure 4.14. Graphical view of the comparison of median pixel intensities of the BNG between groups. The statistical significance level is indicated according to their p values: p<0,001=*** or ###, p<0,01=** or ## and p<0,05=* or #.

The α-Bungarotoxin (BNG) biomarker, which binds to the Acetylcholine receptors and stains them, indicates neuromuscular junction. The pixel intensity of BNG, which binds to a NAR in the neuromuscular junction, was scientifically significantly higher in the sham group in comparison with the crush group (p<0,001). The pixel intensity of BNG was scientifically significantly higher in the HDA 30 group in comparison with the crush group (p<0,001). The pixel intensity of BNG was scientifically significantly higher in the HDA 60 group in comparison with the crush group (p<0,001). The pixel intensity of BNG was scientifically significantly higher in the HDA 60 group in comparison with the HDA 30 group (p<0,01) (Table 4.6, Figure 4.14, and Figure 4.20).

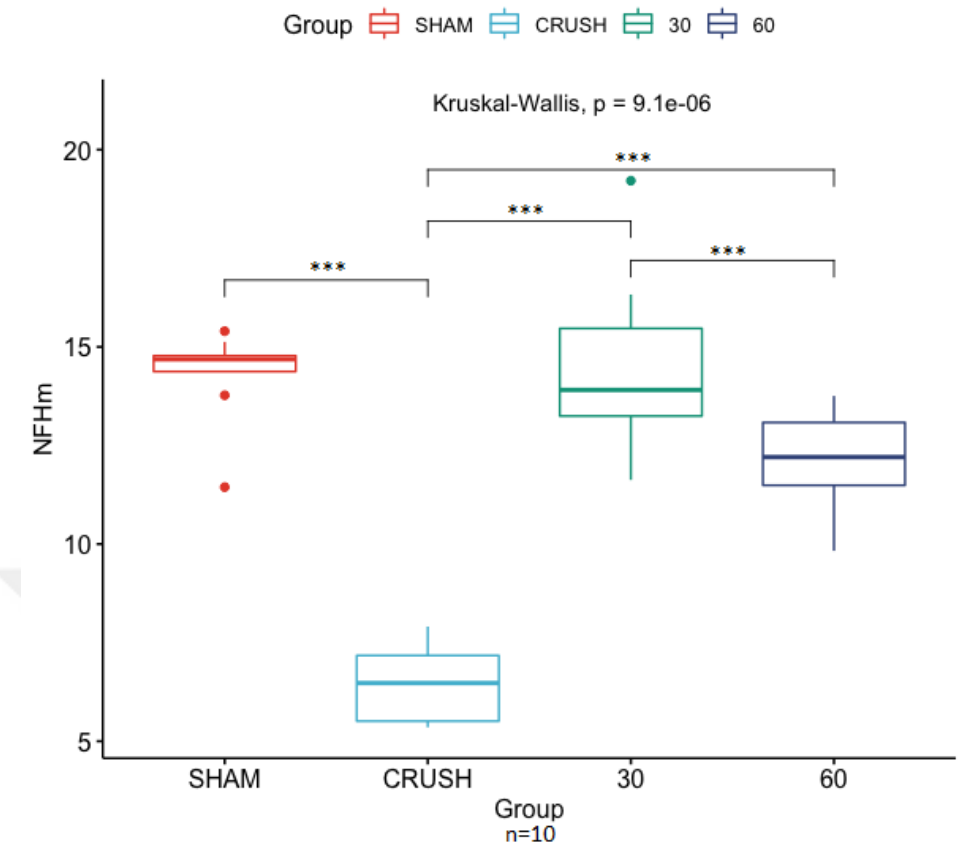

Figure 4.15. Graphical view of the comparison of NFH-M median pixel intensities in muscle specimens. The statistical significance level is indicated according to their p values: p<0,001=*** or ###, p<0,01=** or ## and p<0,05=* or #.

NFH-M in an axon elongates into the gastrocnemius muscle. The pixel intensity of NFH-M was scientifically significantly higher in the sham group in comparison with the crush group (p<0,001). The pixel intensity of NFH-M was scientifically significantly higher in the HDA 30 group in comparison with the crush group (p<0,001). The pixel intensity of NFH-M was scientifically significantly higher in the HDA 60 group in comparison with the crush group (p<0,001). The pixel intensity of NFH-M was scientifically significantly higher in the HDA 30 group in comparison with the HDA 60 group (p<0,001). (Table 4.6, Figure 4.15, and Figure 4.20).

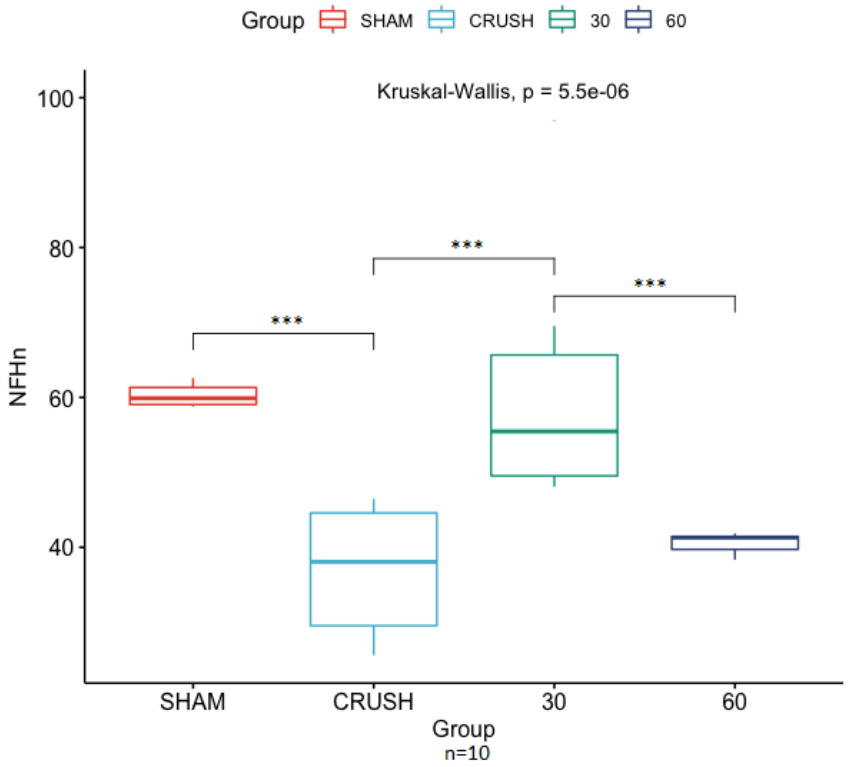

Figure 4.16. Graphical view of the comparison of the nerve NFH median pixel intensities between groups. The statistical significance level is indicated according to their p values: p<0,001=*** or ###, p<0,01=** or ## and p<0,05=* or #.

The pixel intensity of the sciatic nerve section's neurofilament exhibited similarity with NFH-M. The pixel intensity of NFH-N was scientifically significantly higher in the sham group in comparison with the crush group (p<0,001). The pixel intensity of NFH-N was scientifically significantly higher in the HDA 30 group in comparison with the crush group (p<0,001). The pixel intensity of NFH-N was scientifically equal between HDA 60 and crush groups. The pixel intensity of NFH-N was scientifically significantly higher in the HDA 30 group in comparison with the HDA 60 group (p<0,001) (Table 4.6, Figure 4.16, and Figure 4.19).

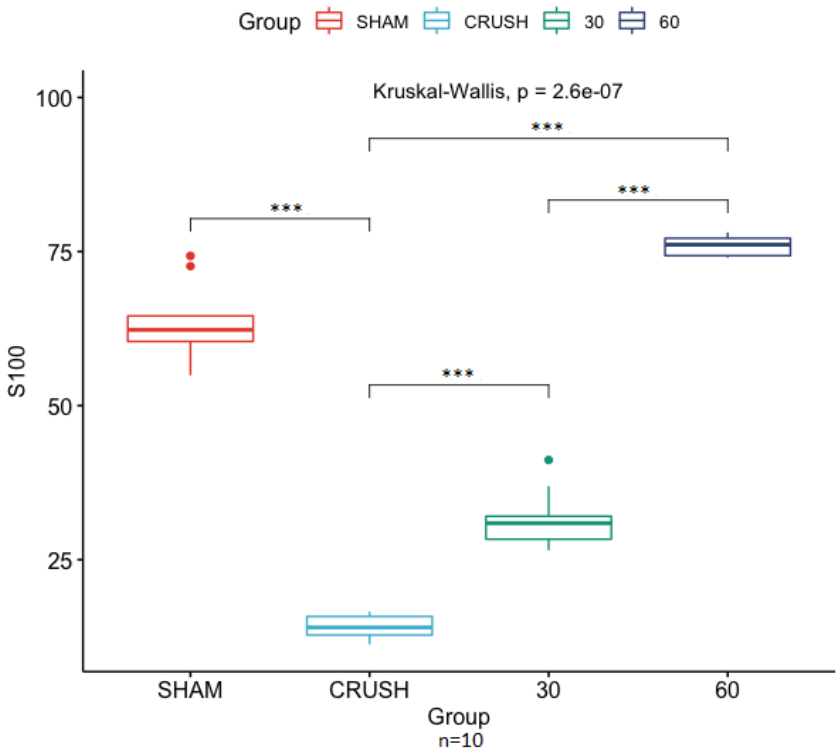

Figure 4.17. Graphical view of the comparison of the S100 median pixel intensities between groups. The statistical significance level is indicated according to their p values: p<0,001=*** or ###, p<0,01=** or ## and p<0,05=* or #.

The pixel intensity of S100 was scientifically significantly higher in the sham group in comparison with the crush group (p<0,001). The pixel intensity of S100 was scientifically significantly higher in the HDA 30 group in comparison with the crush group (p<0,001). The pixel intensity of S100 was scientifically significantly higher in the HDA 60 group in comparison with the crush group (p<0,001). The pixel intensity of S100 was scientifically significantly higher in the HDA 60 group in comparison with the HDA 30 group (p<0,001). (Table 4.6, Figure 4.17, and Figure 4.19).

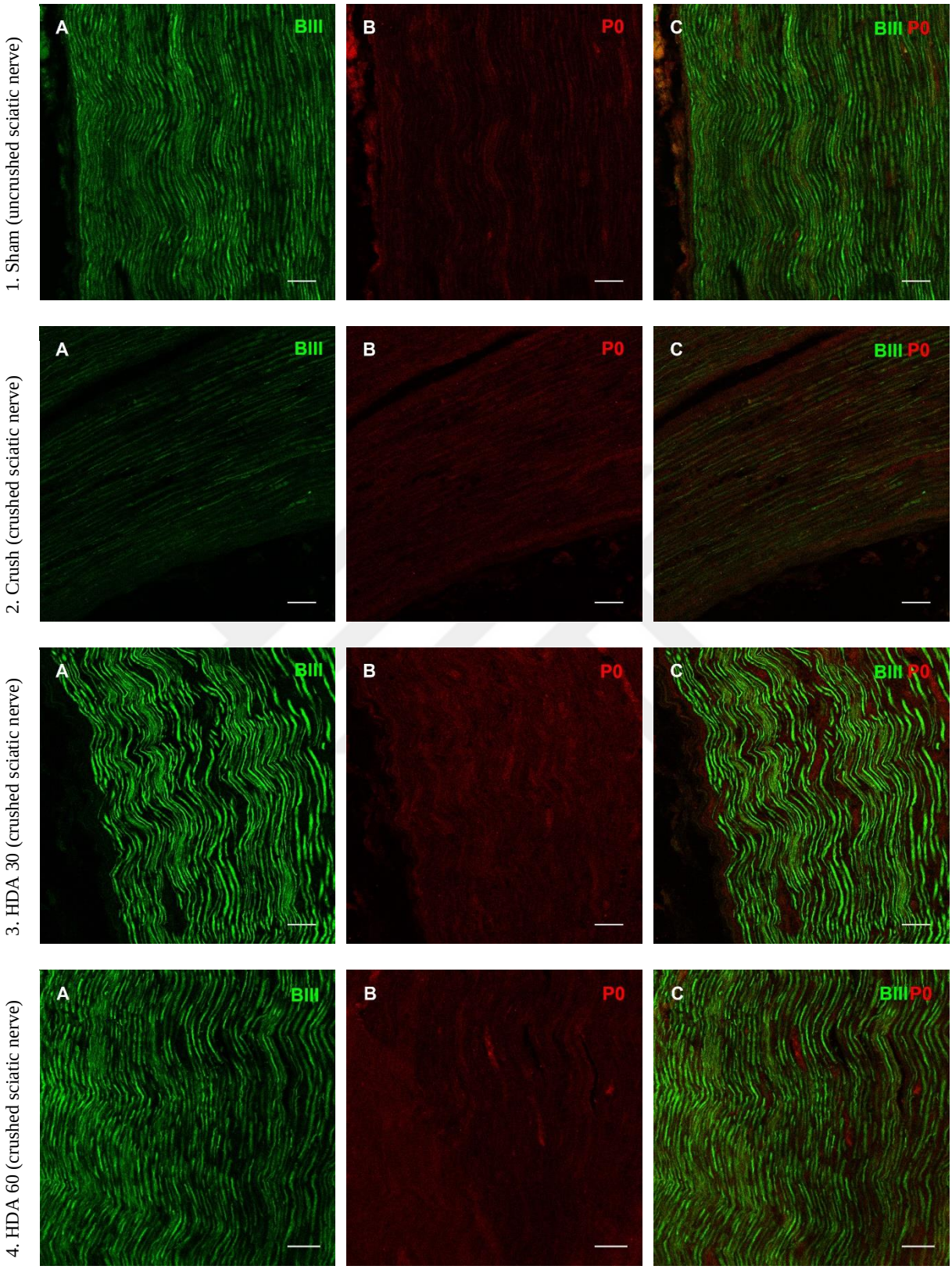

Figure 4.18. Images of immunofluorescence comparison for four groups, sciatic nerve tissue. 1: Sham group, 2: Crush group, 3: HDA 30 treatment group, 4: HDA 60 30 treatment group. A: BIII, B: P0, C: Double Staining with BIII and P0. Scalebar 50 μm.

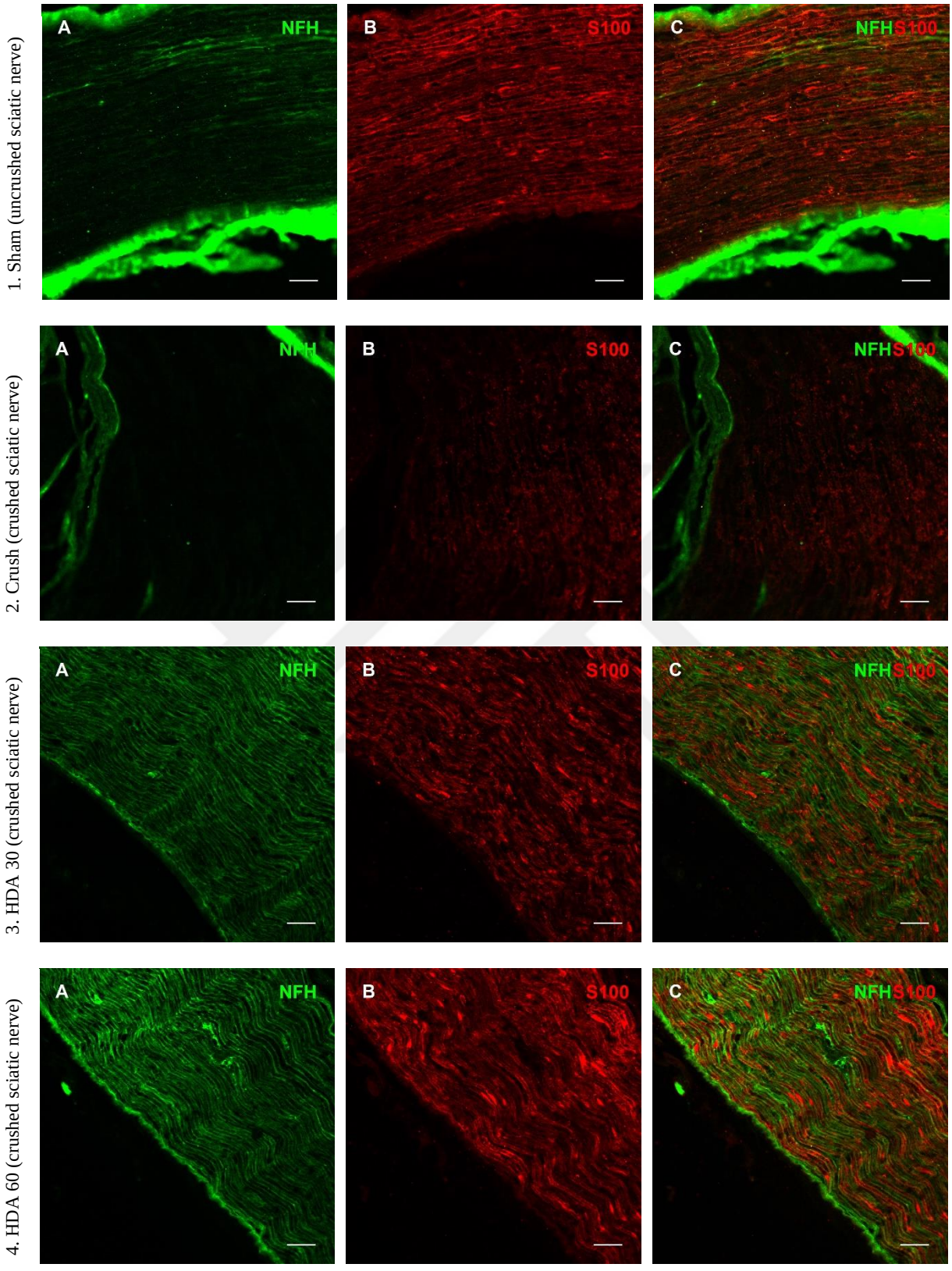

Figure 4.19. Images of immunofluorescence comparison for four groups, sciatic nerve tissue. 1: Sham group, 2: Crush group, 3: HDA 30 treatment group, 4: HDA 60 30 treatment group. A: NFH, B: S100, C: Double Staining with NFH and S100. Scalebar 50 μm.

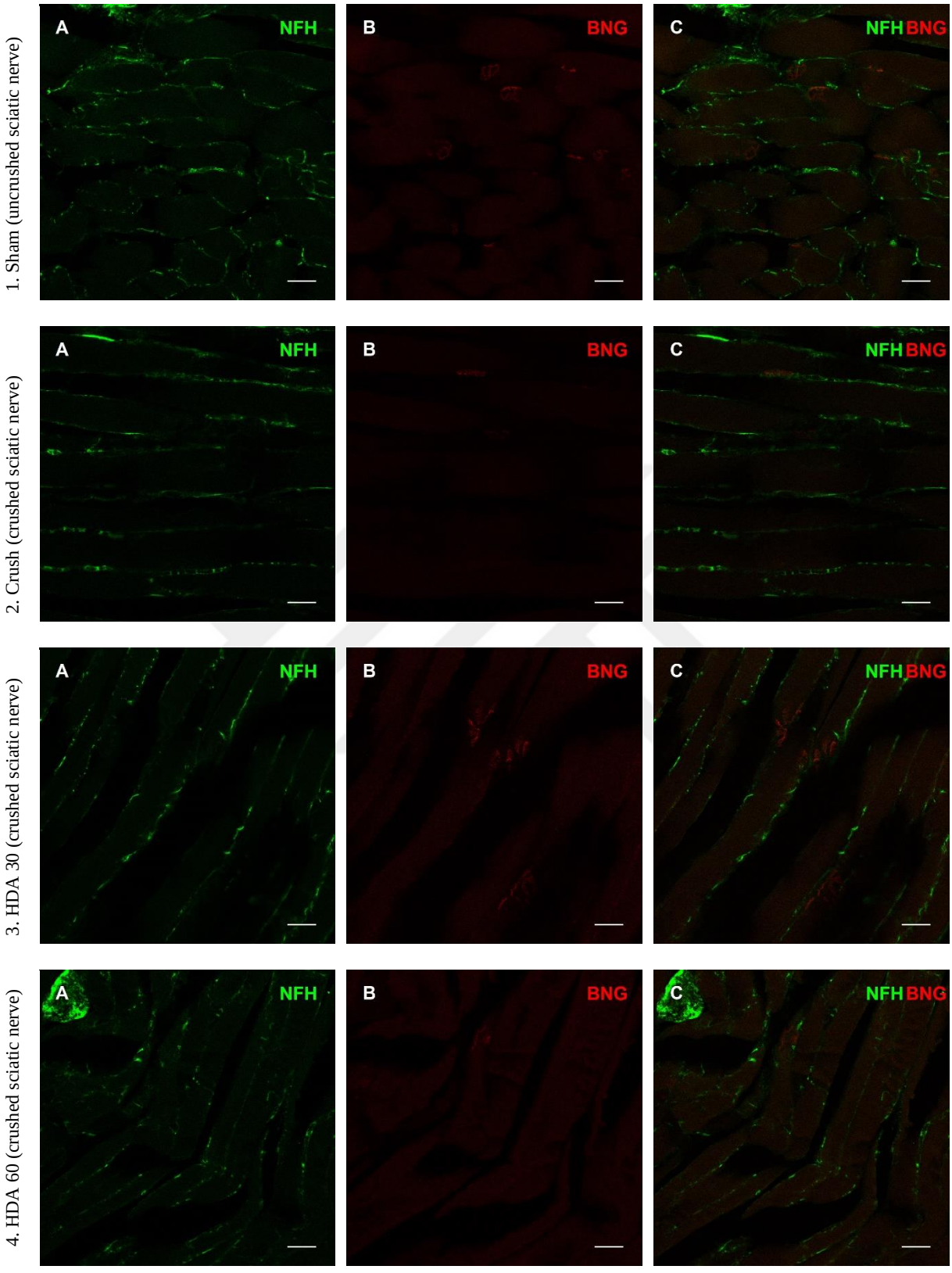

Figure 4.20. Images of immunofluorescence comparison for four groups, Gastrocnemius muscle tissue.

1: Sham group, 2: Crush group, 3: HDA 30 treatment group, 4: HDA 60 30 treatment group.

A: NFH, B: BNG, C: Double Staining with NFH and BNG. Scalebar 50 µm.

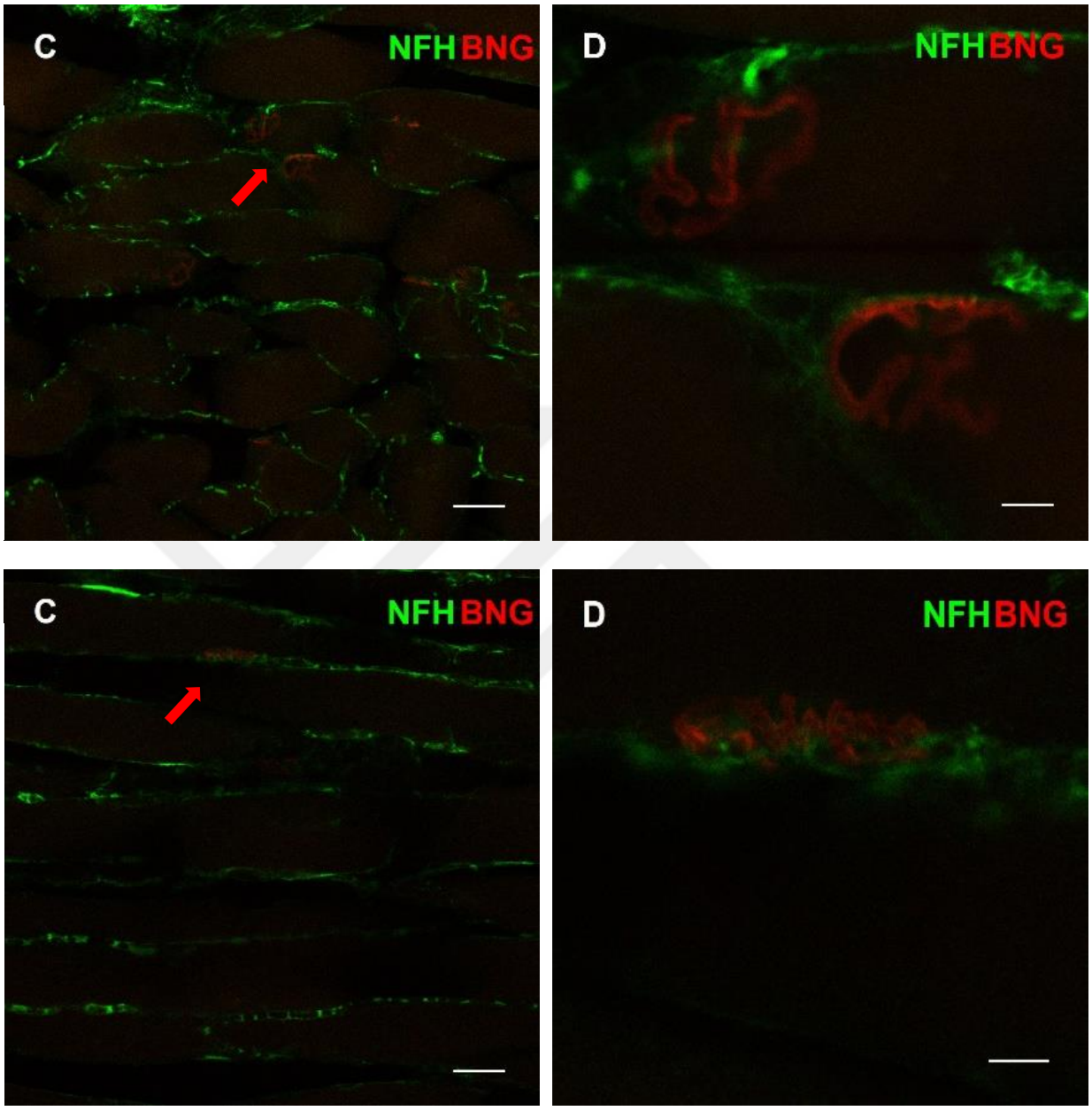
1. Sham (uncrushed sciatic nerve)
C
NFH BNG
D
NFH BNG
2. Crush (crushed sciatic nerve)
C
NFH BNG
D
NFH BNG

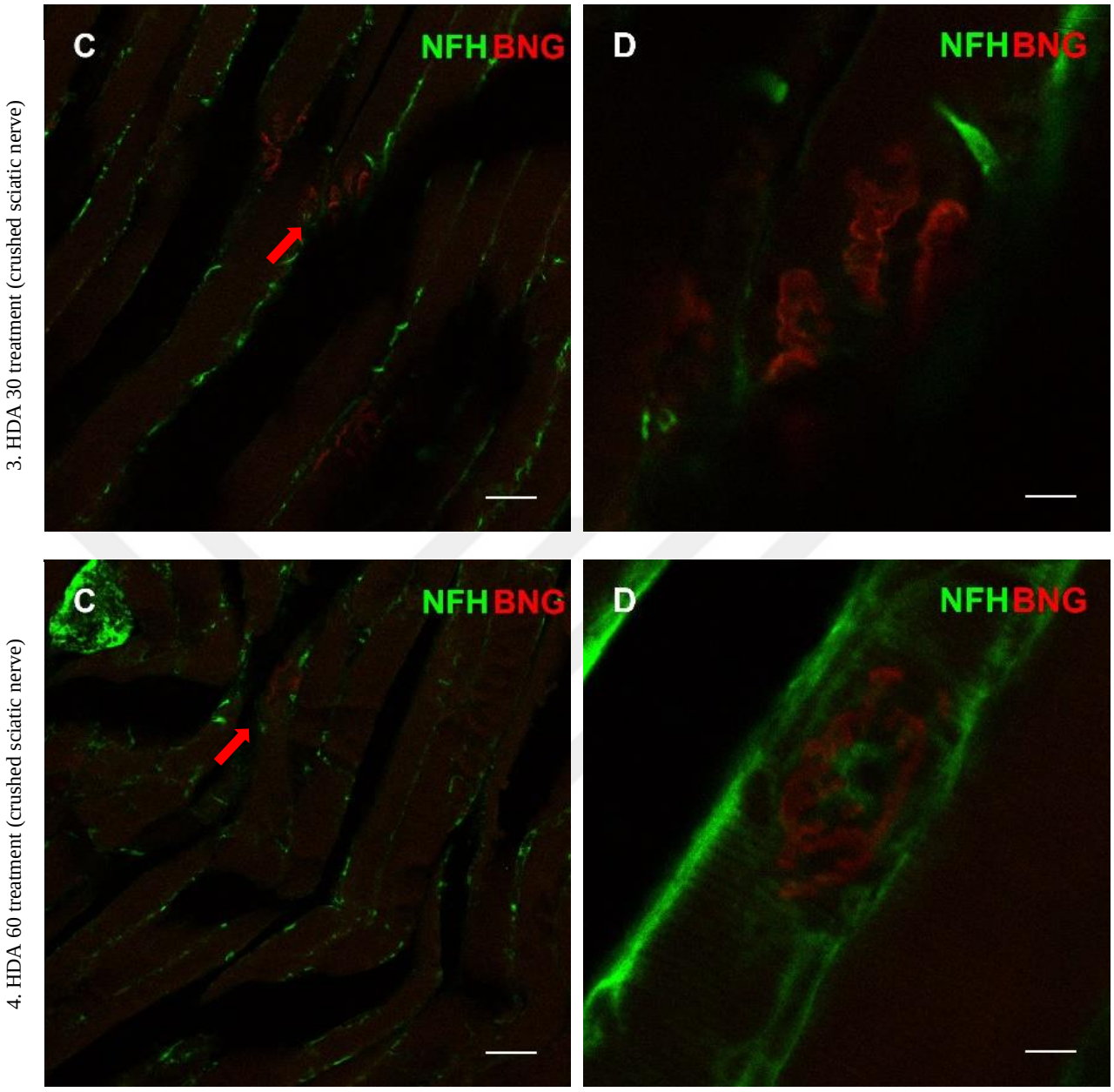

Figure 4.21. Images of immunofluorescence comparison for four groups, Gastrocnemius muscle tissue. Arrows pointing the NAR clusters which have been cropped and magnified.
1: Sham group, 2: Crush group, 3: HDA 30 treatment group, 4: HDA 60 30 treatment group.
C: Double Staining of NFH and BNG, D: Cropped images from Figure C, the NAR's. Scalebar C: 50 μm, D: 10 μm.

5. DISCUSSION AND CONCLUSION

This study aimed to enlighten the regenerative effects of 10-HDA on the sciatic nerve for the first time. The functional tests were proceeded during 30 days of an experimental period. The electromyographic and histometric tests were carried out at the end of the experimental study. The axonal regeneration, myelin sheath repair, reinnervation, and sensory and motor functions were evaluated to see whether the results would support each other. Almost all results were complementary and supportive of each other. The reinnervation studies were also satisfactory.

Mouse sciatic nerve crush injury model is one of the most common experimental models used in the field of regenerative research [128]. The sciatic nerve injury model is commonly being used to enlighten the mechanism of PNI, a common health problem in clinics worldwide [1,129].

Mice were used in this study. Rodents are well-known and used in the nerve regeneration studies due to their highly regenerative capabilities, the ease of their availabilities, the low care and maintenance costs, their tolerance to captivity, and higher resistance to post-surgical infections; yet the advantages and disadvantages between each other (mainly mice and rat) are still being discussed [130]. Several studies/reviews compare these properties and indicate that both rats and mice have similar functional recovery [131], rats have better-regenerating patterns [132], and mice recover faster than rats [131]. We have chosen mice because of their handling ease and highly regenerative capacities. The outstanding reasons why sciatic nerve was chosen to be examined were its; surgery facilitating tissue magnitude, accessible anatomical positioning, and the comparative convenience inflicted by the massive amount of previous pre-clinical data properties [129]. The nerve crush injury is frequently used among other injury methods such as transverse injury, clamp injury, keep epineurium injury, and chemical injury models [133]. We have chosen crush injury because of the less post-operative process, reproducibility, and highly precisive properties.

We decided to use a sham group because we aimed to eliminate the effect of the muscle incision injury that might had inferred with our functional and electrophysiological tests.

5.1. The Efficacy of the Sciatic Nerve Crush Injury in a Mouse Animal Model

The functional tests (Thermal hyperalgesia, SFI, HLRWT, and rotarod tests) performed on day 5 (T1) following injury revealed a statistically significant difference between the sham

and crush groups. This data has confirmed the efficacy of the sciatic nerve crush injury in a mouse model.

Besides, all of the functional test results of T0 tests revealed that the mice had no individual functional difference between each other as there was no statistically significant difference among any groups.

5.2. The Evaluation of the Efficacy of 10-HDA Through the Functional Tests, Electrophysiological Tests and IHC

Before all, this study has shown that the data from all tests complement each other. All the functional tests were made by the same person in this study to prevent any individual deviations. Besides, these are the first functional test results proving the efficacy of 10-HDA treatment according to the literature review.

The thermal hyperalgesia test is a test to evaluate the sensory functions of the sciatic nerve [117]. So many studies have reported the increased thermal hyperalgesia withdrawal latency following the sciatic nerve crush injury [134]. The hyperalgesia arising from the heat causes an evasion reflex in the mice, which can be observed clearly by the naked eye due to the pain (nociceptive) withdrawal reflex. The thermal pain withdrawal reflex arc consists of a sensory receptor (nociceptor), sensory neuron, interneuron, motor neuron, and effector (muscle) organ. The thermal hyperalgesia T1 results indicate that the mice's sciatic nerve degenerates drastically. The sensory part of the sciatic nerve was unable to function after the injury.

The findings of thermal hyperalgesia obtained at T2 showed that the 10-HDA treatment is effective on the 17th day following the injury for both HDA 30 and HDA 60 groups at the same level. This result indicated that the regenerative effect on peripheral nerves of 10 HDA is exceptionally rapid. The results of T3 tests proved that 30 and 60 mg/kg doses of 10-HDA is also effective at 29th day following the injury, however the significance between HDA 30 and crush group decreased in comparison with T2 trials. This indicates that the intrinsic regeneration mechanisms which are independent from the pharmacological intervention healed the crush group, but it still wasn’t faster than the 30 mg/kg does of 10-HDA treatment. The between weeks comparison showed that HDA 60 group had no significant difference between post operative weeks, while HDA 30 group rapidly healed their sensory functions starting from the 17th day of the treatment.

The quantitative method of analyzing hind limbs performance by examining footprints, known as the sciatic function index (SFI), is widely used to quantify functional recovery from

sciatic nerve injury in several different injury models [114,115]. The crush injury on the sciatic nerve affects all the surrounding muscles, creating a disfunction in the walking properties and the foot shape [135]. The shrinkage, which results from contracture or atrophy on the feet, is evident in these results, just like in some other studies [135]. There are so many studies claiming the functional tests are not up to date or do not reflect the actual progress of the regeneration due to a few reasons like the reciprocal compensation mechanisms, the so-called subjective operating differences, auto mutilation, or technical problems like the smearing of the ink for the SFI test [136,137].

According to our results, both 30 and 60 mg/kg doses of 10 HDA gradually healed the kinesthetic properties of the injured mice within the assays. Interestingly, while the T1 tests revealed that 60 mg/kg was the effective dose, the T2 and T3 tests resulted in a better regenerative effect of the 30 mg/kg of dose. Especially T3 tests showed that HDA 30 group had no significant difference from the sham group, which means full recovery on sciatic function index was succeeded. The efficacy of the 60 mg/kg dose for the early recovery might be due to the rapid healing effect of 10-HDA[138] on muscle atrophy caused by crush-induced denervation [139]. The SFI T3 test results indicate that the healing effect of 30 mg/kg of 10-HDA on the SFI is higher than the 60 mg/kg 10-HDA treatment. Consequently, 30 mg/kg of 10-HDA would be the best therapeutical strategy for improving sciatic functions.

The related criticism was made for HLRWT too. Especially the observing problems since the movement details are so unremarkable to be seen by eye, “cross limb transferring” or motor learning of the rungs has been discussed for a while [140]. The critical and specific grading scale (7 in total) is a susceptible method to calculate the full score. Also, motor learning of the rung’s location is a very reasonable point; however, the combination of the rungs was changed before each assay.

The results in T2 of the HLRWT revealed the efficacy of 10-HDA at regeneration on the 17th day following the crush injury. The ladder test helps reveal both the sensory and motor functions of the nerve since the mice must sense the ladder rung it is on at the exact moment and plan the next step by calculating the possible gap to complete the process of the whole ladder. The apparent difference between sham and crush groups results from the motor and sensory dysfunctions [141]. Many studies also indicate the complementary effects of the SFI test and horizontal ladder rung walking test, just like the survey carried out by Ribeiro’s group [141]. The T3 assays showed no statistically significant difference between groups, revealing that the sensory motor functions have recovered rapidly during the regeneration regardless of the pharmacological intervention. This result might also be due to the lack of an incline. Antonow-

Schlaarke and his team revealed that minor modifications detected more specific results when a slight incline was applied to the system [142]. The onboard gravity parameter helps the strength of the muscle to be supervened in the analysis.

T2 and T3 rotarod results showed that 10-HDA treatment had a complete recovery effect in both HDA 30 and HDA 60 groups. Furthermore, this result verified that the regenerative effect on peripheral nerves of 10 HDA is exceptionally rapid. The results revealed that 10-HDA could fully reverse the sensory and motor degenerative effects of crush injury. The faster regeneration of motor functions was also approved by Moldovan [143]. The complementary data of functional tests in this study has been strengthened by the several results made in the same procedure. Cardoso and its team also proved the similarity between SFI and rotarod tests [144].

We evaluated sciatic nerve function and muscle activity using electromyography (EMG) and recorded three parameters: latency, compound muscle action potential (CMAP), and motor conduction velocities. The latency parameter revealed the nerve's degeneration or regeneration, while the CMAP parameter indicated axon degeneration or axon regeneration, and the MNCV reflected the demyelination or remyelination.

The latency measurement results were similar to the functional tests and the IHC results. The latency findings obtained from the EMG tests on the 29th day of the injury revealed that 10-HDA treatment groups had a statistically significant better and faster latency than the crush group.

The CMAP results indicated no statistically significant difference between none of the groups. This might be due to the mice's sciatic nerve axons' having extremely high intrinsic regeneration capacity. The nerve’s electromyographical properties are the fastest to recover compared with the other properties. Yet, the invasive technique used in this study (needle electrodes) prevented the examination from being repeated routinely since the electrodes would harm the feet and cause inflammation.

The impulse's speed in the nerve is determined by myelinization, which consists of myelin sheath and the Schwann cells [48]. Myelination is an essential process that determines the MNCV [145]. MNCV of the HDA 60 group was significantly higher than the crush group. This result is parallel with the increased levels of P0 and S100 at the HDA 30 or HDA 60 groups. The invasive technique used in this study (needle electrodes) prevented the examination from being repeated routinely since the electrodes would harm the feet and cause inflammation [146]. Therefore, the EMG test was only made at the end of the assays, carried out on the 29th day following the injury.

The P0 was very effective for both doses. There was no significant difference between HDA 30 and HDA 60 groups. P0 intensity indicated that morphological completion of myelination in axons. When P0 pixel intensity is discussed with MNCV findings, it was understood that 2 tests were compatible with each other.

The IHC data obtained from BIII revealed that full recovery was unavailable, yet the NFH-N was almost at the same level as the sham group after the 30 mg/kg dose of 10-HDA treatment. This was contradictory to a study that revealed the direct interaction between NFH and the MNCV [147]. The CMAP is a parameter to detect the degeneration on the axon. NFH and the BIII proteins are the main proteins of axon, however CMAP values for each group showed no significant difference. This unexpected result could have been a result of procedural problems; however, we were able to record acceptable and complementary data from the MNCV and latency parameters; therefore, the surrounding muscles' action potentials might have interfered with the CMAP of the gastrocnemius muscle, which also was proposed by Goodman [148] and Griffin [132].

The three stages of our measurements can be lined up from the first step to the last step, such as morphologic (IHC) – electrophysiological (EMG) – functional.

The IHC results provided the precise and most satisfactory data in this study. However, the electrophysiological reflection of this proof might not be seen due to; the time required for the molecular changes to start functioning, the complex procedure, and functions of an action potential or procedural problems. Regarding to such as gain-weighting to the intact leg, increasing the step frequency, and motor learning capability (like holding on the rotarod mile without falling down) the non-compensating tests; the abovementioned atoning neuropathic pain mechanism might have interfered with the actual data. Besides, Dvali has mentioned the struggle to prove the regeneration due to the poor functional test results [149].

Pixel intensities of P0, BIII, BNG, NFH-M, NFH-N, and S100 proteins in the crush group were statistically significantly lower when compared to the sham group. Quantitative analysis of the fluorescence intensities indicated that the crush damage drastically decreases the proteins on the axon, myelin sheath, or the NAR. Furthermore, our results showed similarities with the study made by Geary and his team [116], Gugliandolo's and his team [150], Liu's and his team [151], and Li and his team [152]. All these results prove the accuracy of the sciatic nerve crush model.

The 10-HDA treatment was proven to be effective at producing axon (BIII and NFH results), myelin (P0 results), and NAR proteins (BNG results) for all of the tests. Some assays have shown that 30 mg/kg is efficient, while some assays proved that the 60 mg/kg of dosage is more efficient. There was no previous study to demonstrate that 10-HDA accelerates the P0,

S100, or NAR, which makes this study unique on this point. A study found that an extract of Royal Jelly increases the amount of B-III positive cells in vitro [153], and none studies were found in vivo. There was only 1 study about 10-HDA's effect on NFH, proving that it increases the expression of NFH in the hippocampus of adult rat brain [154] but not on the sciatic nerve nor gastrocnemius muscle.

Regarding BIII, 30 mg/kg of dosage was the best therapeutical strategy as the HDA 30 group had a statistically significant difference from all groups. The interesting part was that HDA 60 therapy did not affect BIII production since the HDA 60 group was at the same statistically significant level as the crush group. It is a well-known fact that higher doses might not always be best therapeutical strategy [155]. The BNG results revealed that 60 mg/kg of 10-HDA is the best dosage for the NAR production. An interesting fact that 10-HDA consists Acetylcholine itself [156] might be the reason why the higher dose has a better effect on receptor production. The muscular NFH production was at the highest level at HDA 30 group. HDA 60 was also effective since it had a statistically significant difference with crush group. The HDA 30 and HDA 60 groups also had a statistically significant difference. The dose and the length of the treatment period was optimal for this protein. About neural NFH, almost the same results were shown with muscular NFH. The only difference was that the crush group of the muscular NFH had much lower NFH which is understandable because the injury was directly applied on the sciatic nerve. It is obvious that a 30 mg/kg dosage of 10-HDA is optimal for NFH production in the muscle. The S100 protein was at the statistically significant highest level in HDA 60 group. This test is an excellent example for the importance of dose determination since 30 mg/kg of 10-HDA was not enough for the reproduction, while 60 mg/kg of 10-HDA caused a production even higher than the first state.

In summary, the results of sensory function, motor function and motor coordination tests, electromyographic examination, and immunohistochemical analysis are compatible. Furthermore, these results revealed that the sciatic nerve crush injury model was successfully implemented. 30 mg/kg of 10-HDA treatment is thought to be the optimal dosage for this model, however, a longer treatment method could have revealed better electrophysiological results.

- Thermal Hyperalgesia: 10-HDA is effective for regeneration at a 30 mg/kg dose.
- SFI: 10-HDA is effective for regeneration at both 30 mg/kg and 60 mg/kg doses, 30 mg/kg has a higher regenerative effect.
- HLRWT: 10-HDA is effective for regeneration; however, it does not have a statistically difference.

- Rotarod: 10-HDA is effective for regeneration at both 30 and 60 mg/kg doses at the same levels.
- EMG: 10-HDA is effective for both 30 mg/kg and 60 mg/kg doses at the same level for the latency parameter. 60 mg/kg dose has a positive effect on MNCV parameter. Both doses don't have an effect on CMAP parameter.
- IHC: 30 mg/kg and 60 mg/kg doses of 10-HDA are both effective for P0 reproduction at the same level. 30 mg/kg dose of 10-HDA is effective for BIII reproduction. 60 mg/kg dose of 10-HDA is effective for NAR reproduction. 30 mg/kg dose of 10-HDA is effective for both muscular and neural NFH reproduction. 60 mg/kg dose of 10-HDA is effective for S100 reproduction.

5.3. The Possible Mechanism of 10-HDA on Nerve Regeneration

There is evidence that RJ facilitates the mRNA expression of NFH and GDNF levels [154], since we have shown that NFH production was increased with 10- HDA treatment, it is possible that 10-HDA has an effect on the genetical reproduction of NFH. GDNF is known to use the PI3K/Akt pathway [157], there is a possible evidence that 10-HDA might be using the PI3K/Akt pathway for the nerve regeneration. There as another study proving that P0 production might be related to the PI3K/Akt pathway [158], and we have found that both 30 mg/kg and 60 mg/kg doses of 10-HDA are effective on the P0 production. The relationship between S100 protein and PI3K/Akt was also found by Corr and its team [159]. These 3 data might be strong evidence that 10-HDA shows its regenerative effects via PI3K/Akt pathway.

Another possible mechanism of 10-HDA contributes the regeneration via inflammatory modulation. A study has shown that HDA modulates IL-8, IL-1β and TNF-α in WiDr cells, it significantly decreases IL-1β and TNF-α and reduces NF-κB [138]. There is evidence that TNF-α uses the JNK pathway which leads the neuron to survive or die [160], it is possible that 10-HDA uses the pro-survival path. There is one evidence that RJ increases the BDNF levels on rats, which uses the TrkB pathway and activates the MEK/Erk pathway [161]. Besides, another study examining the relationship between 10-HDA and estrogen receptors suggested that there might be a slight possibility that 10-HDA uses the MEK/Erk pathway [22]. However, there is no data about the relationship between 10-HDA and BDNF. This can be another possible mechanism which is a note for the future.

5.4. Further Recommendations

Regarding the functional tests, the unexpected results for the horizontal ladder rung walking test indicate that a slight incline should have been applied, which is to note for the future. Regarding the thermal analgesia test results, that is clear that a complementary sensory function test is required to be able to duplicate and cross-check the results before having an opinion on 10-HDA and sensory functions.

A positive control group with a well-known regenerative compound/molecule can be a good reference in order to compare the efficacy of 10-HDA. Besides as 10-HDA is the main ingredient of RJ, it can be useful to include one more group with standardized RJ extract to have an idea about the supra-additive effects of other compounds as a wholesome synergistic effect.

The two from three EMG parameters have resulted in a non-complementary way. Eventually, using a different animal with a lower speed of regenerating capacity (mimicking human regeneration) or expanding the treatment period could allow for a better result. Also, making the assays in a more frequent period can be another option. However, a non-invasive device is required for such a technique.

Some further study about the possible pathways by using the specific biomarkers for NGF receptors or the well-known regeneration signalizing pathways would be an excellent complementary study such as MAPK/ERK, JAK/STAT, etc., besides in vitro study would have been a tremendous source of information about the molecular differences during the regeneration process which are both already in progress.

6. REFERENCES

1. TÜİK Kurumsal. https://data.tuik.gov.tr/Bulten/Index?p=Karayolu-Trafik-Kaza-Istatistikleri-2018-30640. Accessed December 9, 2021.

2. SGK 2009. http://www.sgk.gov.tr/wps/portal/sgk/tr/kurumsal/istatistik/sgk_istatistik_yilliklari. Accessed December 9, 2021.

3. Grinsell D, Keating CP. Peripheral Nerve Reconstruction after Injury: A Review of Clinical and Experimental Therapies. *Biomed Res Int*. 2014;2014. doi:10.1155/2014/698256

4. Zhang YG, Sheng QS, Wang HK, et al. Triptolide improves nerve regeneration and functional recovery following crush injury to rat sciatic nerve. *Neurosci Lett*. 2014;561:198-202. doi:10.1016/j.neulet.2013.12.068

5. TEMİZ NÇ, MEHTİYEV R, KACAR Y, et al. Periferik Sinir Lezyonlarında Prognostik Faktörler ve KlinikSonuçlarımız. *Fırat Tıp Derg*. 2016;21(4):209-213. https://app.trdizin.gov.tr/makale/TWpNM056SXlNZz09/periferik-sinir-lezyonlarinda-prognostik-faktorler-ve-klinik-sonuclarimiz. Accessed February 15, 2021.

6. Farinas AF, Manzanera Esteve I V., Pollins AC, et al. Diffusion Magnetic Resonance Imaging Predicts Peripheral Nerve Recovery in a Rat Sciatic Nerve Injury Model. *Plast Reconstr Surg*. 2020;145(4):949-956. doi:10.1097/PRS.0000000000006638

7. Samadian H, Maleki H, Fathollahi A, et al. Naturally occurring biological macromolecules-based hydrogels: Potential biomaterials for peripheral nerve regeneration. *Int J Biol Macromol*. 2020;154:795-817. doi:10.1016/j.ijbiomac.2020.03.155

8. Sarker MD, Naghieh S, McInnes AD, Schreyer DJ, Chen X. Regeneration of peripheral nerves by nerve guidance conduits: Influence of design, biopolymers, cells, growth factors, and physical stimuli. *Prog Neurobiol*. 2018;171:125-150. doi:10.1016/j.pneurobio.2018.07.002

9. Li R, Li D hui, Zhang H yu, Wang J, Li X kun, Xiao J. Growth factors-based therapeutic strategies and their underlying signaling mechanisms for peripheral nerve regeneration. *Acta Pharmacol Sin*. 2020;41(10):1289-1300. doi:10.1038/s41401-019-0338-1

10. Wanner R, Knöll B. Interference with SRF expression in skeletal muscles reduces peripheral nerve regeneration in mice. *Sci Rep*. 2020;10(1). doi:10.1038/s41598-020-62231-4

11. Scheib J, Höke A. Advances in peripheral nerve regeneration. *Nat Rev Neurol*. 2013;9(12):668-676. doi:10.1038/nrneurol.2013.227

12. Müller M, Wilder S, Bannasch D, et al. p53 activates the CD95 (APO-1/Fas) gene in response to DNA damage by anticancer drugs. *J Exp Med*. 1998;188(11):2033-2045. doi:10.1084/jem.188.11.2033

13. Hart AM, Terenghi G, Wiberg M. Neuronal death after peripheral nerve injury and experimental strategies for neuroprotection. *Neurol Res*. 2008;30(10):999-1011. doi:10.1179/174313208X362479

14. Mahar M, Cavalli V. Intrinsic mechanisms of neuronal axon regeneration. *Nat Rev Neurosci*. 2018;19(6):323-337. doi:10.1038/s41583-018-0001-8

15. Araújo-Filho HG, Quintans-Júnior LJ, Barreto AS, Almeida JRGS, Barreto RSS, Quintans JSS. Neuroprotective Effect of Natural Products on Peripheral Nerve Degeneration: A Systematic Review. *Neurochem Res*. 2016;41(4):647-658. doi:10.1007/s11064-015-1771-2

16. Gordon T, English AW. Strategies to promote peripheral nerve regeneration: Electrical stimulation and/or exercise. *Eur J Neurosci*. 2016;43(3):336-350. doi:10.1111/ejn.13005

17. Borlongan C V. Remyelinating the transected peripheral nerve by fabricated Schwann cells derived from bone marrow. *Exp Neurol*. 2010;225(2):243-245. doi:10.1016/j.expneurol.2010.07.008

18. Pandeya PR, Lamichhane R, Lee KH, et al. Bioassay-guided isolation of active anti-adipogenic compound from royal jelly and the study of possible mechanisms. *BMC Complement Altern Med*. 2019;19(1). doi:10.1186/s12906-018-2423-2

19. Ramadan MF, Al-Ghamdi A. Bioactive compounds and health-promoting properties of royal jelly: A review. *J Funct Foods*. 2012;4(1):39-52. doi:10.1016/j.jff.2011.12.007

20. Pandeya PR, Lamichhane R, Lee KH, et al. Bioassay-guided isolation of active anti-adipogenic compound from royal jelly and the study of possible mechanisms. *BMC Complement Altern Med*. 2019;19(1):33. doi:10.1186/s12906-018-2423-2

21. You M, Pan Y, Liu Y, et al. Royal jelly alleviates cognitive deficits and β-amyloid accumulation in APP/PS1 mouse model via activation of the cAMP/PKA/CREB/BDNF pathway and inhibition of neuronal apoptosis. *Front Aging Neurosci*. 2019;11(JAN). doi:10.3389/fnagi.2018.00428

22. Weiser M, Grimshaw V, Wynalda K, Mohajeri M, Butt C. Long-Term Administration of Queen Bee Acid (QBA) to Rodents Reduces Anxiety-Like Behavior, Promotes Neuronal Health and Improves Body Composition. *Nutrients*. 2017;10(1):13. doi:10.3390/nu10010013

23. Catala M, Kubis N. Gross anatomy and development of the peripheral nervous system. *Handb Clin Neurol*. 2013;115:29-41. doi:10.1016/B978-0-444-52902-2.00003-5

24. Chen Z-L, Yu W-M, Strickland S. Peripheral Regeneration. 2007. doi:10.1146/annurev.neuro.30.051606.094337

25. ML W, M R, JG G, PK B. Peripheral nerve injury, scarring, and recovery. *Connect Tissue Res*. 2019;60(1):3-9. doi:10.1080/03008207.2018.1489381

26. Andrews MG, Kong J, Novitch BG, Butler SJ. New perspectives on the mechanisms establishing the dorsal-ventral axis of the spinal cord. *Curr Top Dev Biol*. 2019;132:417-450. doi:10.1016/BS.CTDB.2018.12.010

27. Neuroscience: Exploring the brain, 3rd ed. - PsycNET. https://psycnet.apa.org/record/2007-18995-000. Accessed September 9, 2021.

28. L L, WC X, L M. Neuromuscular Junction Formation, Aging, and Disorders. *Annu Rev Physiol*. 2018;80:159-188. doi:10.1146/ANNUREV-PHYSIOL-022516-034255

29. MF E, R M, M H, T D. Unique Characteristics of the Dorsal Root Ganglion as a Target for Neuromodulation. *Pain Med*. 2019;20(Suppl 1):S23-S30. doi:10.1093/PM/PNZ012

30. Herophilus. Ein Beitrag zur Geschichte der Medicin - Carl Friedrich Heinrich Marx - Google Kitaplar. https://books.google.com.tr/books?hl=tr&lr=&id=bV1OAAAAcAAJ&oi=fnd&pg=PA2&ots=UFXhDPDE90&sig=VkeBHWZZru7i6QJtmqP_FpbrE_0&redir_esc=y#v=onepage&q&f=false. Accessed August 5, 2021.

31. The Seven Books of Paulus Aegineta: Translated from the Greek, with a ... - Paulus (Aegineta.), Francis Adams - Google Kitaplar. https://books.google.com.tr/books?hl=tr&lr=&id=4b0s40WeNcQC&oi=fnd&pg=PR5&ots=hcqLxSK5ea&sig=YeTBw5HIr_5eJLjr87qM6-IGCFs&redir_esc=y#v=onepage&q&f=false. Accessed August 5, 2021.

32. Walters BC. History of Peripheral Nerve Repair. *Nerves Nerve Inj*. 2015:23-36. doi:10.1016/B978-0-12-410390-0.00002-0

33. Eser F, Aktekin LA, Bodur H, Dem Atan Ç. Etiological factors of traumatic peripheral nerve injuries. 57. doi:10.4103/0028-3886.55614

34. Menorca RMG, Fussell TS, Elfar JC. Nerve Physiology Mechanisms of Injury and Recovery. 2013. doi:10.1016/j.hcl.2013.04.002

35. ML W, M R, JG G, PK B. Peripheral nerve injury, scarring, and recovery. *Connect Tissue Res*. 2019;60(1):3-9. doi:10.1080/03008207.2018.1489381

36. MG B, EL Z. Pathophysiology of peripheral nerve injury: a brief review. *Neurosurg Focus*. 2004;16(5). doi:10.3171/FOC.2004.16.5.2

37. G S, S J, RR M. Degeneration and regeneration of the peripheral nervous system: from Augustus Waller's observations to neuroinflammation. *J Peripher Nerv Syst*. 2002;7(1):13-27. doi:10.1046/J.1529-8027.2002.02002.X

38. Stoll G, Griffin JW, Li CY, Trapp BD. Wallerian degeneration in the peripheral nervous system: participation of both Schwann cells and macrophages in myelin degradation. *J Neurocytol 1989 185*. 1989;18(5):671-683. doi:10.1007/BF01187086

39. WW S, RP B. Effects of calcium ion concentration on the degeneration of amputated axons in tissue culture. *J Cell Biol*. 1973;59(2 Pt 1):456-470. doi:10.1083/JCB.59.2.456

40. Rosales C, Uribe-Querol E. Phagocytosis: A Fundamental Process in Immunity. 2017. doi:10.1155/2017/9042851

41. Weiss P, Wang H. Transformation of Adult Schwann Cells Into Macrophages.*: *https://doi.org/103181/00379727-58-14920*. 2016;58(4):273-275. doi:10.3181/00379727-58-14920

42. Brosius Lutz A, Chung W-S, Sloan SA, et al. Schwann cells use TAM receptor-mediated phagocytosis in addition to autophagy to clear myelin in a mouse model of nerve injury. doi:10.1073/pnas.1710566114

43. Napoli I, Noon LA, Ribeiro S, et al. A central role for the ERK-signaling pathway in controlling Schwann cell plasticity and peripheral nerve regeneration in vivo. *Neuron*. 2012;73(4):729-742. doi:10.1016/J.NEURON.2011.11.031

44. Ma CHE, Omura T, Cobos EJ, et al. Accelerating axonal growth promotes motor recovery after peripheral nerve injury in mice. *J Clin Invest*. 2011;121(11):4332-4347. doi:10.1172/JCI58675

45. Lu P, Wang Y, Graham L, et al. Long-distance growth and connectivity of neural stem cells after severe spinal cord injury. *Cell*. 2012;150(6):1264-1273. doi:10.1016/J.CELL.2012.08.020

46. Hanz S, Perlson E, Willis D, et al. Axoplasmic Importins Enable Retrograde Injury Signaling in Lesioned Nerve. *Neuron*. 2003;40(6):1095-1104. doi:10.1016/S0896-6273(03)00770-0

47. Tom VJ, Steinmetz MP, Miller JH, Doller CM, Silver J. Development/Plasticity/Repair Studies on the Development and Behavior of the Dystrophic Growth Cone, the Hallmark of Regeneration Failure, in an In Vitro Model of the Glial Scar and after Spinal Cord Injury. 2004. doi:10.1523/JNEUROSCI.0994-04.2004

48. Kandel ER, Koester J, Mack S, Siegelbaum S. Patterning The Nervous System. *Princ neural Sci*. 2021:1107-1129. https://www.mhprofessional.com/9781259642234-usa-principles-of-neural-science-sixth-edition-group. Accessed November 28, 2021.

49. Bradke F, Fawcett JW, Spira ME. Assembly of a new growth cone after axotomy: the precursor to axon regeneration. *Nat Publ Gr*. 2012;13. doi:10.1038/nrn3176

50. Chierzi S, Ratto GM, Verma P, Fawcett JW. The ability of axons to regenerate their growth cones depends on axonal type and age, and is regulated by calcium, cAMP and ERK. *Eur J Neurosci*. 2005;21(8):2051-2062. doi:10.1111/J.1460-9568.2005.04066.X

51. Ziv NE, Spira ME. Axotomy induces a transient and localized elevation of the free intracellular calcium concentration to the millimolar range. *J Neurophysiol*. 1995;74(6):2625-2637. doi:10.1152/JN.1995.74.6.2625

52. Spira ME, Benbassat D, Dormann A. Resealing of the proximal and distal cut ends of transected axons: Electrophysiological and ultrastructural analysis. *J Neurobiol*. 1993;24(3):300-316. doi:10.1002/neu.480240304

53. Sahly I, Khoutorsky A, Erez H, Prager-Khoutorsky M, Spira ME. On-line confocal imaging of the events leading to structural dedifferentiation of an axonal segment into a growth cone after axotomy. *J Comp Neurol*. 2006;494(5):705-720. doi:10.1002/CNE.20690

54. Gitler D, Spira ME. Real time imaging of calcium-induced localized proteolytic activity after axotomy and its relation to growth cone formation. *Neuron*. 1998;20(6):1123-1135. doi:10.1016/S0896-6273(00)80494-8

55. Myers JP, Gomez TM. Focal Adhesion Kinase Promotes Integrin Adhesion Dynamics Necessary for Chemotropic Turning of Nerve Growth Cones. *J Neurosci*. 2011;31(38):13585. doi:10.1523/JNEUROSCI.2381-11.2011

56. Suter DM, Miller KE. The Emerging Role of Forces in Axonal Elongation. *Prog Neurobiol*. 2011;94(2):91. doi:10.1016/J.PNEUROBIO.2011.04.002

57. Rhee J, Mahfooz NS, Arregui C, Lilien J, Balsamo J, VanBerkum MFA. Activation of the repulsive receptor roundabout inhibits N-cadherin-mediated cell adhesion. *Nat Cell Biol*. 2002;4(10):798-805. doi:10.1038/NCB858

58. Liu G, Beggs H, Jürgensen C, et al. Netrin requires focal adhesion kinase and Src family kinases for axon outgrowth and attraction. *Nat Neurosci*. 2004;7(11):1222-1232. doi:10.1038/NN1331

59. Ren XR, Ming GL, Xie Y, et al. Focal adhesion kinase in netrin-1 signaling. *Nat Neurosci*. 2004;7(11):1204-1212. doi:10.1038/NN1330

60. Castellani V, De Angelis E, Kenwrick S, Rougon G. Cis and trans interactions of L1 with neuropilin-1 control axonal responses to semaphorin 3A. *EMBO J*. 2002;21(23):6348-6357. doi:10.1093/EMBOJ/CDF645

61. Barberis D, Artigiani S, Casazza A, et al. Plexin signaling hampers integrin-based adhesion, leading to Rho-kinase independent cell rounding, and inhibiting lamellipodia extension and cell motility. *FASEB J*. 2004;18(3):592-594. doi:10.1096/FJ.03-0957FJE

62. Valdembri D, Caswell PT, Anderson KI, et al. Neuropilin-1/GIPC1 signaling regulates alpha5beta1 integrin traffic and function in endothelial cells. *PLoS Biol*. 2009;7(1). doi:10.1371/JOURNAL.PBIO.1000025

63. Seerapu HR, Borthakur S, Kong N, et al. The cytoplasmic domain of neuropilin-1 regulates focal adhesion turnover. *FEBS Lett*. 2013;587(21):3392-3399. doi:10.1016/J.FEBSLET.2013.08.040

64. Blexrud MD, Lee DA, Windebank AJ, Brunden KR. Kinetics of production of a novel growth factor after peripheral nerve injury. *J Neurol Sci*. 1990;98(2-3):287-299. doi:10.1016/0022-510X(90)90270-W

65. Lu P, Tuszynski MH. Growth factors and combinatorial therapies for CNS regeneration. *Exp Neurol*. 2008;209(2):313-320. doi:10.1016/J.EXPNEUROL.2007.08.004

66. Cui Q. Actions of neurotrophic factors and their signaling pathways in neuronal survival and axonal regeneration. *Mol Neurobiol*. 2006;33(2):155-179. doi:10.1385/MN:33:2:155

67. Hallböök F. Evolution of the vertebrate neurotrophin and Trk receptor gene families. *Curr Opin Neurobiol*. 1999;9(5):616-621. doi:10.1016/S0959-4388(99)00011-2

68. Fahnestock M, Yu G, Michalski B, et al. The nerve growth factor precursor proNGF exhibits neurotrophic activity but is less active than mature nerve growth factor. *J Neurochem*. 2004;89(3):581-592. doi:10.1111/J.1471-4159.2004.02360.X

69. Huang EJ, Reichardt LF. Trk receptors: roles in neuronal signal transduction. *undefined*. 2003;72:609-642. doi:10.1146/ANNUREV.BIOCHEM.72.121801.161629

70. Reichardt LF. Neurotrophin-regulated signalling pathways. *Philos Trans R Soc B Biol Sci*. 2006;361(1473):1545. doi:10.1098/RSTB.2006.1894

71. Friedman WJ, Greene LA. Neurotrophin Signaling via Trks and p75. *Exp Cell Res*. 1999;253(1):131-142. doi:10.1006/EXCR.1999.4705

72. Miller FD, Kaplan DR. Neurotrophin signalling pathways regulating neuronal apoptosis. *Cell Mol Life Sci C 2001 588*. 2001;58(8):1045-1053. doi:10.1007/PL00000919

73. Levi-Montalcini R. The nerve growth factor: thirty-five years later. *EMBO J*. 1987;6(5):1145-1154. doi:10.1002/J.1460-2075.1987.TB02347.X

74. Yun YR, Won JE, Jeon E, et al. Fibroblast growth factors: Biology, function, and application for tissue regeneration. *J Tissue Eng*. 2010;1(1):1-18. doi:10.4061/2010/218142

75. Abbott NJ, Rönnbäck L, Hansson E. Astrocyte-endothelial interactions at the blood-brain barrier. *Nat Rev Neurosci*. 2006;7(1):41-53. doi:10.1038/NRN1824

76. Grothe C, Jungnickel J, Haastert K. Physiological role of basic FGF in peripheral nerve development and regeneration: potential for reconstruction approaches. *Futur Neurol*. 2008;3(5):605-612. doi:10.2217/14796708.3.5.605

77. Choi DY, Toledo-Aral JJ, Lin HY, et al. Fibroblast growth factor receptor 3 induces gene expression primarily through Ras-independent signal transduction pathways. *J Biol Chem*. 2001;276(7):5116-5122. doi:10.1074/JBC.M002959200

78. Slavin BR, Sarhane KA, von Guionneau N, et al. Insulin-Like Growth Factor-1: A Promising Therapeutic Target for Peripheral Nerve Injury. *Front Bioeng Biotechnol*. 2021;9:549. doi:10.3389/FBIOE.2021.695850/BIBTEX

79. Chang YM, Chang HH, Tsai CC, et al. Alpinia oxyphylla Miq. fruit extract activates IGFR-PI3K/Akt signaling to induce Schwann cell proliferation and sciatic nerve regeneration. *BMC Complement Altern Med*. 2017;17(1). doi:10.1186/S12906-017-1695-2

80. Meier C, Parmantier E, Brennan A, Mirsky R, Jessen KR. Developing Schwann cells acquire the ability to survive without axons by establishing an autocrine circuit involving insulin-like growth factor, neurotrophin-3, and platelet-derived growth factor-BB. *J Neurosci*. 1999;19(10):3847-3859. doi:10.1523/JNEUROSCI.19-10-03847.1999

81. Lobsiger C, Schweitzer B, Taylor V, Suter U. Platelet-derived growth factor-BB supports the survival of cultured rat schwann cell precursors in synergy with neurotrophin-3. *undefined*. 2000. doi:10.1002/(SICI)1098-1136(200005)30:3

82. Hohn A, Leibrock J, Bailey K, Barde YA. Identification and characterization of a novel member of the nerve growth factor/brain-derived neurotrophic factor family. *Nature*. 1990;344(6264):339-341. doi:10.1038/344339A0

83. Rosenthal A, Goeddel D V., Nguyen T, et al. Primary structure and biological activity of a novel human neurotrophic factor. *Neuron*. 1990;4(5):767-773. doi:10.1016/0896-6273(90)90203-R

84. Klein R, Nanduri V, Jing S, et al. The trkB tyrosine protein kinase is a receptor for brain-derived neurotrophic factor and neurotrophin-3. *Cell*. 1991;66(2):395-403. doi:10.1016/0092-8674(91)90628-C

85. Sahenk Z, Nagaraja HN, McCracken BS, et al. NT-3 promotes nerve regeneration and sensory improvement in CMT1A mouse models and in patients. *Neurology*. 2005;65(5):681-689. doi:10.1212/01.WNL.0000171978.70849.C5

86. D'Angelo L, Avallone L, Cellerino A, et al. Neurotrophin-4 in the brain of adult Nothobranchius furzeri. *Ann Anat*. 2016;207:47-54. doi:10.1016/J.AANAT.2016.02.005

87. Omura T, Sano M, Omura K, et al. Different expressions of BDNF, NT3, and NT4 in muscle and nerve after various types of peripheral nerve injuries. *J Peripher Nerv Syst*. 2005;10(3):293-300. doi:10.1111/J.1085-9489.2005.10307.X

88. Yin QI, Kemp GJ, Yu L-G, Wagstaff SC, Frostick SP. NEUROTROPHIN-4 DELIVERED BY FIBRIN GLUE PROMOTES PERIPHERAL NERVE REGENERATION. 2001.

89. Richner M, Ulrichsen M, Elmegaard SL, Dieu R, Pallesen LT, Vaegter CB. Peripheral nerve injury modulates neurotrophin signaling in the peripheral and central nervous system. *Mol Neurobiol*. 2014;50(3):945-970. doi:10.1007/S12035-014-8706-9

90. Lee R, Kermani P, Teng KK, Hempstead BL. Regulation of cell survival by secreted proneurotrophins. *Science (80-)*. 2001;294(5548):1945-1948. doi:10.1126/SCIENCE.1065057/SUPPL_FILE/1065057S1_THUMB.GIF

91. Chen ZY, Patel PD, Sant G, et al. Variant brain-derived neurotrophic factor (BDNF) (Met66) alters the intracellular trafficking and activity-dependent secretion of wild-type BDNF in neurosecretory cells and cortical neurons. *J Neurosci*. 2004;24(18):4401-4411. doi:10.1523/JNEUROSCI.0348-04.2004

92. Mizisin AP, Vu Y, Shuff M, Calcutt NA. Ciliary Neurotrophic Factor Improves Nerve Conduction and Ameliorates Regeneration Deficits in Diabetic Rats. *Diabetes*. 2004;53(7):1807-1812. doi:10.2337/DIABETES.53.7.1807

93. Höke A, Ho T, Crawford TO, LeBel C, Hilt D, Griffin JW. Glial Cell Line-Derived Neurotrophic Factor Alters Axon Schwann Cell Units and Promotes Myelination in Unmyelinated Nerve Fibers. *J Neurosci*. 2003;23(2):561-567. doi:10.1523/JNEUROSCI.23-02-00561.2003

94. Cintrón-Colón AF, Almeida-Alves G, Boynton AM, Spitsbergen JM. GDNF synthesis, signaling, and retrograde transport in motor neurons. *Cell Tissue Res*. 2020;382(1):47. doi:10.1007/S00441-020-03287-6

95. Tao T, Ji Y, Cheng C, et al. Tumor necrosis factor-alpha inhibits Schwann cell proliferation by up-regulating Src-suppressed protein kinase C substrate expression. *J Neurochem*. 2009;111(3):647-655. doi:10.1111/J.1471-4159.2009.06346.X

96. Uncini A, Di Muzio A, Di Guglielmo G, et al. Effect of rhTNF-alpha injection into rat sciatic nerve. *J Neuroimmunol*. 1999;94(1-2):88-94. doi:10.1016/S0165-5728(98)00229-X

97. Shamash S, Reichert F, Rotshenker S. The cytokine network of Wallerian degeneration: tumor necrosis factor-alpha, interleukin-1alpha, and interleukin-1beta. *J Neurosci*. 2002;22(8):3052-3060. doi:10.1523/JNEUROSCI.22-08-03052.2002

98. MacEwan DJ. TNF receptor subtype signalling: differences and cellular consequences. *Cell Signal*. 2002;14(6):477-492. doi:10.1016/S0898-6568(01)00262-5

99. Schäfers M, Sorkin L. Effect of cytokines on neuronal excitability. *Neurosci Lett*. 2008;437(3):188-193. doi:10.1016/J.NEULET.2008.03.052

100. Einheber S, Hannocks MJ, Metz CN, Rifkin DB, Salzer JL. Transforming growth factor-beta 1 regulates axon/Schwann cell interactions. *J Cell Biol*. 1995;129(2):443-458. doi:10.1083/JCB.129.2.443

101. Rogister B, Delrée P, Leprince P, et al. Transforming growth factor beta as a neuronoglial signal during peripheral nervous system response to injury. *J Neurosci Res*. 1993;34(1):32-43. doi:10.1002/JNR.490340105

102. Frost HK, Kodama A, Ekström P, Dahlin LB. G-CSF prevents caspase 3 activation in Schwann cells after sciatic nerve transection, but does not improve nerve regeneration. *Neuroscience*. 2016;334:55-63. doi:10.1016/j.neuroscience.2016.07.045

103. Villiger PM, Geng Y, Lotz M. Induction of cytokine expression by leukemia inhibitory factor. *J Clin Invest*. 1993;91(4):1575-1581. doi:10.1172/JCI116363

104. Ostasov P, Houdek Z, Cendelin J, Kralickova M. Role of leukemia inhibitory factor in the nervous system and its pathology. doi:10.1515/revneuro-2014-0086

105. Ito T, Ikeda K, Tomita K, Yokoyama S. Interleukin-6 upregulates the expression of PMP22 in cultured rat Schwann cells via a JAK2-dependent pathway. *Neurosci Lett*. 2010;472(2):104-108. doi:10.1016/J.NEULET.2010.01.061

106. Gaudet AD, Popovich PG, Ramer MS. Wallerian degeneration: gaining perspective on inflammatory events after peripheral nerve injury. *J Neuroinflammation*. 2011;8. doi:10.1186/1742-2094-8-110

107. Hama T, Kushima Y, Miyamoto M, Kubota M, Takei N, Hatanaka H. Interleukin-6 improves the survival of mesencephalic catecholaminergic and septal cholinergic neurons from postnatal, two-week-old rats in cultures. *Neuroscience*. 1991;40(2):445-452. doi:10.1016/0306-4522(91)90132-8

108. Jones SA, Scheller J, Rose-John S. Therapeutic strategies for the clinical blockade of IL-6/gp130 signaling. *J Clin Invest*. 2011;121(9):3375-3383. doi:10.1172/JCI57158

109. You M, Pan Y, Liu Y, et al. Royal jelly alleviates cognitive deficits and β-amyloid accumulation in APP/PS1 mouse model via activation of the cAMP/PKA/CREB/BDNF pathway and inhibition of neuronal apoptosis. *Front Aging Neurosci*. 2019;11(JAN). doi:10.3389/fnagi.2018.00428

110. Cazorla M, Prémont J, Mann A, Girard N, Kellendonk C, Rognan D. Identification of a low-molecular weight TrkB antagonist with anxiolytic and antidepressant activity in mice. *J Clin Invest*. 2011;121(5):1846-1857. doi:10.1172/JCI43992

111. Paredes-Barquero M, Niso-Santano M, Fuentes JM, Martínez-Chacón G. In vitro and in vivo models to study the biological and pharmacological properties of queen bee acid (QBA, 10-hydroxy-2-decenoic acid): A systematic review. *J Funct Foods*. 2022;94:105143. doi:10.1016/J.JFF.2022.105143

112. Almeer RS, Alarifi S, Alkahtani S, Ibrahim SR, Ali D, Moneim A. The potential hepatoprotective effect of royal jelly against cadmium chloride-induced hepatotoxicity in mice is mediated by suppression of oxidative stress and upregulation of Nrf2 expression. *Biomed Pharmacother*. 2018;106:1490-1498. doi:10.1016/j.biopha.2018.07.089

113. Chung DDL. Cement-Matrix Composites. *Carbon Compos*. 2017:333-386. doi:10.1016/B978-0-12-804459-9.00006-3

114. Watadani R, Kotoh J, Sasaki D, Someya A, Matsumoto K, Maeda A. 10-Hydroxy-2-decenoic acid, a natural product, improves hyperglycemia and insulin resistance in obese/diabetic KK-Ay mice, but does not prevent obesity. *J Vet Med Sci*. 2017;79(9):1596-1602. doi:10.1292/jvms.17-0348

115. Sugiyama M, Ito T, Furukawa T, Hirayama A, Kakehata S. The effect of insulin-like growth factor 1 on the recovery of facial nerve function in a guinea pig model of facial palsy. *J Physiol Sci*. 2020;70(1). doi:10.1186/s12576-020-00755-0

116. Geary MB, Li H, Zingman A, et al. Erythropoietin accelerates functional recovery after moderate sciatic nerve crush injury. *Muscle and Nerve*. 2017;56(1):143-151. doi:10.1002/mus.25459

117. Üstün R, Oğuz EK, Delilbaşı Ç, et al. Neuromuscular degenerative effects of Ankaferd Blood Stopper® in mouse sciatic nerve model. *Somatosens Mot Res*. 2017;34(4):248-257. doi:10.1080/08990220.2017.1421160

118. Inserra MM, Bloch DA, Terris DJ. Functional indices for sciatic, peroneal, and posterior tibial nerve lesions in the mouse. *Microsurgery*. 1998;18(2):119-124. doi:10.1002/(SICI)1098-2752(1998)18:2<119::AID-MICR10>3.0.CO;2-0

119. Metz GA, Whishaw IQ. The ladder rung walking task: A scoring system and its practical application. *J Vis Exp*. 2009;(28). doi:10.3791/1204

120. Farr TD, Liu L, Colwell KL, Whishaw IQ, Metz GA. Bilateral alteration in stepping pattern after unilateral motor cortex injury: a new test strategy for analysis of skilled limb movements in neurological mouse models. *J Neurosci Methods*. 2006;153(1):104-113. doi:10.1016/J.JNEUMETH.2005.10.011

121. Harauma A, Tomita M, Muto D, Moriguchi T. Effect of long-term administration of arachidonic acid on n-3 fatty acid deficient mice. *Prostaglandins, Leukot Essent Fat Acids*. 2015;95:41-45. doi:10.1016/j.plefa.2014.12.004

122. Tuffaha SH, Budihardjo JD, Sarhane KA, et al. Growth Hormone Therapy Accelerates Axonal Regeneration, Promotes Motor Reinnervation, and Reduces Muscle Atrophy following Peripheral Nerve Injury. *Plast Reconstr Surg*. 2016;137(6):1771-1780. doi:10.1097/PRS.0000000000002188

123. Namgung U, Choi BH, Park S, et al. Activation of cyclin-dependent kinase 5 is involved in axonal regeneration. *Mol Cell Neurosci*. 2004;25(3):422-432. doi:10.1016/J.MCN.2003.11.005

124. Lim EMF, Nakanishi ST, Hoghooghi V, et al. AlphaB-crystallin regulates remyelination after peripheral nerve injury. *Proc Natl Acad Sci U S A*. 2017;114(9):E1707-E1716. doi:10.1073/pnas.1612136114

125. McLean NA, Popescu BF, Gordon T, Zochodne DW, Verge VMK. Delayed nerve stimulation promotes axon-protective neurofilament phosphorylation, accelerates immune cell clearance and enhances remyelination in vivo in focally demyelinated nerves. *PLoS One*. 2014;9(10). doi:10.1371/JOURNAL.PONE.0110174

126. Xu J, Wen J, Fu L, et al. Macrophage-specific RhoA knockout delays Wallerian degeneration after peripheral nerve injury in mice. *J Neuroinflammation*. 2021;18(1):1-17. doi:10.1186/S12974-021-02292-Y/FIGURES/9

127. O'Sullivan SA, Dev KK. The chemokine fractalkine (CX3CL1) attenuates H2O2-induced demyelination in cerebellar slices. *J Neuroinflammation*. 2017;14(1). doi:10.1186/s12974-017-0932-4

128. Jager SB, Ronchi G, Vaegter CB, Geuna S. The Mouse Median Nerve Experimental Model in Regenerative Research. *Biomed Res Int*. 2014;2014. doi:10.1155/2014/701682

129. Geuna S. The sciatic nerve injury model in pre-clinical research. *J Neurosci Methods*. 2015;243:39-46. doi:10.1016/J.JNEUMETH.2015.01.021

130. Mohanty CB, Bhat DI, Devi B. Use of animal models in peripheral nerve surgery and research. *Neurol India*. 2019;67(7):100. doi:10.4103/0028-3886.250706

131. Vogelaar CF, Vrinten DH, Hoekman MFM, Brakkee JH, Burbach JPH, Hamers FPT. Sciatic nerve regeneration in mice and rats: recovery of sensory innervation is followed by a slowly retreating neuropathic pain-like syndrome. *Brain Res*. 2004;1027(1-2):67-72. doi:10.1016/J.BRAINRES.2004.08.036

132. Griffin JW, Pan BH, Polley MA, Hoffman PN, Farah MH. Measuring nerve regeneration in the mouse. *Exp Neurol*. 2010;223(1):60-71. doi:10.1016/J.EXPNEUROL.2009.12.033

133. Siwei Q, Ma N, Wang W, et al. Construction and effect evaluation of different sciatic nerve injury models in rats. *Transl Neurosci*. 2022;13(1):38. doi:10.1515/TNSCI-2022-0214

134. Li L, Li Y, Fan Z, et al. Ascorbic Acid Facilitates Neural Regeneration After Sciatic Nerve Crush Injury. *Front Cell Neurosci*. 2019;13. doi:10.3389/FNCEL.2019.00108

135. Wang T, Ito A, Aoyama T, et al. Functional evaluation outcomes correlate with histomorphometric changes in the rat sciatic nerve crush injury model: A comparison between sciatic functional index and kinematic analysis. *PLoS One*. 2018;13(12). doi:10.1371/JOURNAL.PONE.0208985

136. Munro CA, Szalai JP, Mackinnon SE, Midha R. Lack of association between outcome measures of nerve regeneration. *Muscle and Nerve*. 1998;21(8):1095-1097. doi:10.1002/(SICI)1097-4598(199808)21:8<1095::AID-MUS20>3.0.CO;2-S

137. Dellon AL, Mackinnon SE. Sciatic nerve regeneration in the rat. Validity of walking track assessment in the presence of chronic contractures. *Microsurgery*. 1989;10(3):220-225. doi:10.1002/MICR.1920100316

138. Yang YC, Chou WM, Widowati DA, Lin IP, Peng CC. 10-hydroxy-2-decenoic acid of royal jelly exhibits bactericide and anti-inflammatory activity in human colon cancer cells. *BMC Complement Altern Med*. 2018;18(1). doi:10.1186/S12906-018-2267-9

139. Urso ML. Anti-inflammatory interventions and skeletal muscle injury: benefit or detriment? *J Appl Physiol*. 2013;115(6):920-928. doi:10.1152/JAPPLPHYSIOL.00036.2013

140. Eisdorfer JT, Phelan MA, Keefe KM, et al. Addition of angled rungs to the horizontal ladder walking task for more sensitive probing of sensorimotor changes. *PLoS One*. 2021;16(2):e0246298. doi:10.1371/JOURNAL.PONE.0246298

141. Ribeiro T, Oliveira JT, Almeida FM, et al. Blockade of ATP P2X7 receptor enhances ischiatic nerve regeneration in mice following a crush injury. *Brain Res*. 2017;1669:69-78. doi:10.1016/J.BRAINRES.2017.05.025

142. Antonow-Schlorke I, Ehrhardt J, Knieling M. Modification of the ladder rung walking task - New options for analysis of skilled movements. *Stroke Res Treat*. 2013. doi:10.1155/2013/418627

143. Moldovan M, Sørensen J, Krarup C. Comparison of the fastest regenerating motor and sensory myelinated axons in the same peripheral nerve. *Brain*. 2006;129(Pt 9):2471-2483. doi:10.1093/BRAIN/AWL184

144. Soares dos Santos Cardoso F, Cardoso R, dos Santos Ramalho B, et al. Inosine Accelerates the Regeneration and Anticipates the Functional Recovery after Sciatic Nerve Crush Injury in Mice. *Neuroscience*. 2019;423:206-215. doi:10.1016/J.NEUROSCIENCE.2019.09.023

145. Waxman SG. Determinants of conduction velocity in myelinated nerve fibers. *Muscle Nerve*. 1980;3(2):141-150. doi:10.1002/MUS.880030207

146. Barry DM, Stevenson W, Bober BG, et al. Expansion of Neurofilament Medium C Terminus Increases Axonal Diameter Independent of Increases in Conduction Velocity or Myelin Thickness. *J Neurosci*. 2012;32(18):6209. doi:10.1523/JNEUROSCI.0647-12.2012

147. Kilpatrick TJ, Tubridy N. Molecular mechanisms regulating motor neuron development and degeneration. *Handb Clin Neurophysiol*. 2004;4(C):97-118. doi:10.1016/S1567-4231(04)04005-5

148. Goodman BP, Harper CM, Boon AJ. Prolonged compound muscle action potential duration in critical illness myopathy. *Muscle and Nerve*. 2009;40(6):1040-1042. doi:10.1002/MUS.21445

149. Dvali L, Mackinnon S. The Role of Microsurgery in Nerve Repair and Nerve Grafting. *Hand Clin*. 2007;23(1):73-81. doi:10.1016/J.HCL.2007.02.003

150. Gugliandolo E, D'Amico R, Cordaro M, et al. Effect of PEA-OXA on neuropathic pain and functional recovery after sciatic nerve crush 11 Medical and Health Sciences 1109 Neurosciences. *J Neuroinflammation*. 2018;15(1):1-13. doi:10.1186/S12974-018-1303-5/FIGURES/6

151. Liu L, Tian D, Liu C, Yu K, Bai J. Metformin enhances functional recovery of peripheral nerve in rats with sciatic nerve crush injury. *Med Sci Monit*. 2019;25:10067-10076. doi:10.12659/MSM.918277

152. Li R, Li D, Wu C, et al. Nerve growth factor activates autophagy in Schwann cells to enhance myelin debris clearance and to expedite nerve regeneration. 10(4):1649-1677. doi:10.7150/thno.40919

153. Hattori N, Nomoto H, Fukumitsu H, Mishima S, Furukawa S. Royal jelly and its unique fatty acid, 10-hydroxy-trans-2-decenoic acid, promote neurogenesis by neural stem/progenitor cells in vitro. *Biomed Res*. 2007;28(5):261-266. doi:10.2220/BIOMEDRES.28.261

154. Hashimoto M, Kanda M, Ikeno K, et al. Oral administration of royal jelly facilitates mRNA expression of glial cell line-derived neurotrophic factor and neurofilament H in the hippocampus of the adult mouse brain. *Biosci Biotechnol Biochem*. 2005;69(4):800-805. doi:10.1271/BBB.69.800

155. Santer P, Eikermann M. High-dose midodrine is not effective for treatment of persistent hypotension in the intensive care unit. *Intensive Care Med*. 2021;47(2):252-253. doi:10.1007/S00134-020-06333-7

156. Ali AM, Kunugi H. Apitherapy for Parkinson's Disease: A Focus on the Effects of Propolis and Royal Jelly. *Oxid Med Cell Longev*. 2020;2020. doi:10.1155/2020/1727142

157. Bahlakeh G, Rahbarghazi R, Mohammadnejad D, Abedelahi A, Karimipour M. Current knowledge and challenges associated with targeted delivery of neurotrophic factors into the central nervous system: focus on available approaches. *Cell Biosci*. 2021;11(1). doi:10.1186/S13578-021-00694-2

158. Liang G, Cline GW, Macica CM. IGF-1 stimulates de novo fatty acid biosynthesis by Schwann cells during myelination. *Glia*. 2007;55(6):632-641. doi:10.1002/GLIA.20496

159. Corr EM, Cunningham CC, Dunne A. Cholesterol crystals activate Syk and PI3 kinase in human macrophages and dendritic cells. *Atherosclerosis*. 2016;251:197-205. doi:10.1016/J.ATHEROSCLEROSIS.2016.06.035

160. A. Frankola K, H. Greig N, Luo W, Tweedie D. Targeting TNF-Alpha to Elucidate and Ameliorate Neuroinflammation in Neurodegenerative Diseases. *CNS Neurol Disord - Drug Targets*. 2011;10(3):391-403. doi:10.2174/187152711794653751

161. Dehbozorgi A, Tabrizi LB, Hosseini SA, Rasoli MH. Effects of Swimming Training and Royal Jelly on BDNF and NGF Gene Expression in Hippocampus Tissue of Rats with Alzheimer's Disease. *Zahedan J Res Med Sci 2020 222*. 2020;22(2):98310. doi:10.5812/ZJRMS.98310

7. APPENDICES

7.1. Appendix: Ethical Approval Form

Evrak Tarih ve Sayısı: 02.03.2021-24781

KİŞİYE ÖZEL

T.C.
VAN YÜZÜNCÜ YIL ÜNİVERSİTESİ REKTÖRLÜĞÜ
Hayvan Deneyleri Yerel Etik Kurulu

Sayı : E-27552122-604.01.02-24781
Konu : Doç. Dr. Ramazan ÜSTÜN'e ait
Araştırma Başvuru Onay Belgesi

Sayın Doç. Dr. Ramazan ÜSTÜN

Hayvan Deneyleri Yerel Etik Kurulu'nun 25/02/2021 tarih ve 2021/02-11 sayılı kararı gereği; Yürütücülüğünü yapmayı tasarladığınız, "Siyatik Sinir Crush Hasarı Oluşturulmuş Farelerde 10-Hidroksi-2- Desenoik Asidin Rejeneratif Etkisinin Morfolojik ve Fonksiyonel Olarak Değerlendirilmesi" adlı projeye raportör değerlendirme sonucuna göre Van YUHADYEK tarafından 01.03.2022 tarihine kadar izin verilmiştir. Çalışmaya başlamadan en az 3 (üç) gün öncesinden denetleyicilerle irtibata geçmeniz gerekmektedir.

Projeye denetleyici olarak Tıp Fakültesi'nden Dr. Öğr. Üyesi Oruç YUNUSOĞLU ve Deney Hayvanları Merkezi'nden Doç. Dr. Yıldıray BAŞBUĞAN görevlendirilmiştir.

Çalışmanın kesin sonuç raporunun zamanında sunulmasından ve bundan kaynaklanacak her türlü aksaklıktan proje yürütücüsü sorumludur.

Gereğini bilgilerinize rica ederim.

Prof. Dr. Semiha DEDE
Etik Kurulu Başkanı

Ek: Doç. Dr. Ramazan ÜSTÜN 11 (1 sayfa)

Bu belge, güvenli elektronik imza ile imzalanmıştır.
Belge Doğrulama Kodu :BELCL786B Pin Kodu :73491 Belge Takip Adresi : https://www.turkiye.gov.tr/vyy-ebys
Adres:Van Yüzüncü Yıl Üniversitesi Hayvan Deneyleri Yerel Etik Kurulu Zeve Kampüsü 65080 Tuşba/ Van
Telefon No: +90 432 22 51701-04 / +90 444 5065 Faks No:+90 432 4865413
e-Postayuhadyek@yyu.edu.tr İnternet Adresi:http://www.yyu.edu.tr
Bilgi için: Mehmet Şah OĞUZ
Unvanı: Şef
Tel No: 22007

KİŞİYE ÖZEL

Bu belge, güvenli elektronik imza ile imzalanmıştır.

7.2. Appendix: Research Final Report Approval Certificate

VAN YÜHADYEK
VAN YÜZÜNCÜ YIL ÜNİVERSİTESİ
Hayvan Deneyleri Yerel Etik Kurulu

ARAŞTIRMA KESİN SONUÇ ONAY BELGESİ

VAN YUZUNCUYILUNIVERSITY (TURKEY)
ANIMAL RESEARCHES LOCAL ETHIC COMMITTEE
RESEARCH FINAL REPORT APPROVAL CERTIFICATE

Araştırmanın Adı *Research Title*	Siyatik Sinir Crush Hasarı Oluşturulmuş Farelerde 10-hidroksi-2-desenoik Asidin Rejeneratif Etkisinin Morfolojik ve Fonksiyonel Olarak Değerlendirilmesi Morphological and Functional Evaluation of the Regenerative Effect of 10-hydroxy-2-decenoic Acid in Mice with Sciatic Nerve Crush Injury	
Araştırıcı(lar) *Investigator(s)*	**Yürütücü** / *Chief investigator :*	Doç. Dr. Ramazan Üstün
	Yardımcı Araştırıcı(lar) / *Co-investigator(s):*	Arş. Gör. R. Sena Türker

Araştırmanın Başlama Tarihi / *Research Starting Date:* 30.03.2021

Araştırmanın Bitiş Tarihi / *Research Completion Date:* 30.03.2022

Proje Süresi / *Total Time of Project:* 12 ay

Proje No / *Project Number:* TDK-2021-9481

Araştırmayı Destekleyen Kuruluş (varsa)/ *Funding institution(s) (if available):* VAN YYÜ BAP

Destek Şekli ve Miktarı / *Type and amount of funding:* Doktora Projesi / 25.000

Karar:
Yukarıda bilgileri verilen araştırma projesinin kesin sonuç raporu Van Yüzüncü Yıl Üniversitesi Hayvan Deneyleri Yerel Etik Kurulu'nun 26/05/2022 tarih ve 2022/05-26 sayılı kararı ile kabul edilmiştir.
Decision:
Final report of the research project detailed above was approved by Van Yuzuncu Yil University Animal Researches Local Ethic Committee in the session held on 26/05/2022 (decision number 2022/05-26

	BAŞKAN/CHAIR Prof. Dr. Semiha DEDE	
ÜYE/Member Prof. Dr. N. Tuğba BİNGÖL	**ÜYE/Member** Prof. Dr. Sıddık KESKİN	**ÜYE/Member** Prof. Dr. Nalan ÖZDAL
ÜYE Prof. Dr. Atilla DURMUŞ	**ÜYE/Member** Doç. Dr. Ferda KARAKUŞ	**ÜYE/Member** Doç. Dr. Yıldıray BAŞBUĞAN
ÜYE/Member Doç. Dr. Cüneyt Yılmaz DEMİR	**ÜYE/Member** Doç. Dr. Abdulahad DOĞAN	**ÜYE/Member** Dr. Öğr. Üyesi Dicle ALTINDAL
ÜYE/Member Dr. Öğr. Üyesi Şükrü ONALAN	**ÜYE/Member** Vet. Hek. İsmail Hakkı BEHÇET	**ÜYE/Member** Zir. Müh. Kenan YILDIRIMOĞLU

8. CURRICULUM VITAE

Personal Information

First Name	Rabia Sena	**Last Name**	Türker
Place of Birth			
Nationality			
E-mail			

Educational Status

Degree	**Field**	**Name of the Graduated Institution**	**Graduation Year**
Doctorate			
Postgraduate			
University	Faculty of Pharmacy	Marmara University	2014
High School			

Foreign Language	**Foreign Language Exam Score**
English	YÖKDİL: 90 (05.03.2017)

Work Experience

Job	**Institution**	**Time (Year – Year)**
Research assistant	Van Yuzuncu Yil University Pharmacology Department	2014-

Computer skills

Program	**Ability to use**
MS Office	Medium

Scientific **Studies**

Articles published in journals included in SCI, SSCI, AHCI

Articles published in other journals

Regenerative capacity of mesenchymal stem cells in peripheral nerve injury crush model. Üstün, R., Oğuz, EK., Akkoca, T., Şeker, A., Türker, RS., Keskin, S. Anatomy: International Journal of Experimental & Clinical Anatomy. 2020 Supplement, Vol. 14, pS118-S119. 2p.
Biological activities and chemical composition of Xanthoria lichens from Turkey. Mükemre, M., Zengin, G., Türker, RS., Aslan, A., Dalar, A. Volume 8, Issue 4, 376 - 388, 26.12.2021

Papers presented at international scientific meetings and published in the proceedings book

Siyatik sinir crush hasarı oluşturulmuş farelerde 10-hidroksi-2-desenoik asidin rejeneratif etkisinin fonksiyonel olarak değerlendirilmesi (The Functional Evaluation Of 10-Hydroxy-2-Decenoic Acid's Regenerative Effect on Mice with Sciatic Nerve Crush Model) – Türker, RS., Üstün R., Yılmaz, B., Şeker, A. 19th National Neuroscience Congress, Turkey 2021
Koronavirüsün Beyne Yolculuğu (The Adventure of Coronavirus Through the Brain) – 5. Uluslarası Uygulamalı Bilimler Kongresi. Türker, RS. Diyarbakır Turkey, 2020
Antiepileptic Folk Medicines from Eastern Anatolia. Turker, RS., Dalar, A., Allahverdiyev, O. - 2nd International Conference on Natural Products Utilization Plovdiv/SOFIA, 2015
The Folk Medicinal Plants Of Çatak Bulut, G., Tuzlaci, E., Türker, R.S. - 4th International Meeting on Pharmacy & Pharmaceutical Sciences, Istanbul, 2014

Other (Projects/Certificates/Awards)

Yeditepe University International Laboratory Animal Science Course Certificate - 2016